

Lawrence Berkeley National Laboratory

Recent Work

Title

SOME PROPERTIES OF Σ^+ AND Σ^0 HYPERONS PRODUCED IN K-p INTERACTIONS BETWEEN 1.05 AND 1.7 BeV/c

Permalink

<https://escholarship.org/uc/item/2b85v05b>

Authors

Berge, J. Peter
Eberhard, Philippe
Hubbard, J. Richard
et al.

Publication Date

1965-09-03

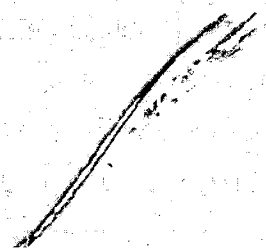
University of California
Ernest O. Lawrence
Radiation Laboratory

TWO-WEEK LOAN COPY

*This is a Library Circulating Copy
which may be borrowed for two weeks.
For a personal retention copy, call
Tech. Info. Division, Ext. 5545*

**SOME PROPERTIES OF Ξ^- AND Ξ^0 HYPERONS PRODUCED IN
 K^-p INTERACTIONS BETWEEN 1.05 AND 1.7 BeV/c**

Berkeley, California



DISCLAIMER

This document was prepared as an account of work sponsored by the United States Government. While this document is believed to contain correct information, neither the United States Government nor any agency thereof, nor the Regents of the University of California, nor any of their employees, makes any warranty, express or implied, or assumes any legal responsibility for the accuracy, completeness, or usefulness of any information, apparatus, product, or process disclosed, or represents that its use would not infringe privately owned rights. Reference herein to any specific commercial product, process, or service by its trade name, trademark, manufacturer, or otherwise, does not necessarily constitute or imply its endorsement, recommendation, or favoring by the United States Government or any agency thereof, or the Regents of the University of California. The views and opinions of authors expressed herein do not necessarily state or reflect those of the United States Government or any agency thereof or the Regents of the University of California.

Reprinted from THE PHYSICAL REVIEW, Vol. 147, No. 4, 945-961, 29 July 1966
 Printed in U. S. A.

Some Properties of Ξ^- and Ξ^0 Hyperons Produced in K^-p Interactions between 1.05 and 1.7 BeV/c*

J. PETER BERGE, PHILIPPE EBERHARD, J. RICHARD HUBBARD, DEANE W. MERRILL,
 J. BUTTON-SHAFER, FRANK T. SOLMITZ, AND M. LYNN STEVENSON
 Lawrence Radiation Laboratory, University of California, Berkeley, California

(Received 29 November 1965)

The production of cascade hyperons by incident K^- on hydrogen has been studied from threshold (1.05 BeV/c) to 1.7 BeV/c. A sample of 1004 Ξ^- and 206 Ξ^0 was obtained. Production cross sections rise over this momentum range, reaching about 150 μb for Ξ^-K^+ production and about 100 μb each for Ξ^0K^0 and $\Xi\pi K$. Production of the $\Xi^*(1530)$ near threshold is observed, and the assignment $I=\frac{1}{2}$ for this resonance is confirmed. The Ξ decay analysis yields weak evidence for $J_{\Xi}=\frac{1}{2}$. For $J_{\Xi}=\frac{1}{2}$, our decay-parameter results are $\alpha_{\Xi^-}=-0.368\pm 0.057$ and $\Phi_{\Xi^-}=\tan^{-1}(\beta/\gamma)_{\Xi}=0.008\pm 0.186$ rad. The final-state $\pi\Lambda$ phase difference is then $(\delta_P-\delta_S)=\tan^{-1}(\beta/\alpha)_{\Xi}=179\pm 26$ deg. No significant violation of the $\Delta I=\frac{1}{2}$ rule was observed. The upper limit on the leptonic decay rate, $(\Xi^- \rightarrow \Lambda e^- \nu)/(\Xi^- \rightarrow \Lambda \pi^-)$, was found to be 0.5%.

I. INTRODUCTION

WE report here results of an analysis of the decay and production properties of cascade hyperons applied to a sample of 1004 Ξ^- and 206 Ξ^0 events observed in an exposure of the Lawrence Radiation Laboratory's 72-in. hydrogen bubble chamber to an incident K^- beam ranging in momentum from the Ξ threshold (1.05 BeV/c) to 1.7 BeV/c. Preliminary results based on partial analyses of various fractions of these data have appeared previously; no substantial modification of earlier results is required by completion of this work.¹⁻⁴

Section II outlines the selection criteria, event-analysis procedures, and corrections applied to the data. The production properties of the ΞK and $\Xi K\pi$ systems are presented in Secs. III and IV. Sections V and VI detail the decay investigation. We find some evidence for the Ξ^- spin to be $\frac{1}{2}$, and give values for the nonleptonic decay parameters α , β , and γ , defined according to a consistent convention,⁵ to higher statistical precision than before. Upper limits on the Ξ^- and Ξ^0 leptonic decay rates are presented. In the conclusion, our results are compared to some predictions of the SU_3 model of strong interactions.

* This work was done under the auspices of the U. S. Atomic Energy Commission.

¹ L. W. Alvarez, J. P. Berge, G. R. Kalbfleisch, J. Button-Shafer, F. T. Solmitz, M. L. Stevenson, and H. K. Ticho, in *Proceedings of the 1962 Conference on High Energy Physics at CERN* (CERN, Geneva, 1962), p. 433.

² J. R. Hubbard, J. P. Berge, G. R. Kalbfleisch, J. B. Shafer, F. T. Solmitz, M. L. Stevenson, S. G. Wojcicki, and P. G. Wohlmut, *Phys. Rev.* **135**, B183 (1964).

³ M. L. Stevenson, J. P. Berge, J. R. Hubbard, G. R. Kalbfleisch,

J. B. Shafer, F. T. Solmitz, S. G. Wojcicki, and P. G. Wohlmut, *Phys. Letters* **9**, 349 (1964).

⁴ M. Ferro-Luzzi, M. H. Alston, A. H. Rosenfeld, and S. G. Wojcicki, *Phys. Rev.* **130**, 1568 (1963).

⁵ It is known that T. D. Lee and C. N. Yang [*Phys. Rev.* **108**, 1645 (1957)] and J. Cronin and O. Overseth (Ref. 22) have an inconsistency in the definition of β ; their definitions of β from the decay amplitudes and the condition imposed by time-reversal invariance should be read with an opposite sign.

TABLE I. Numbers of events and channel cross sections. Cross sections have been corrected for scanning efficiency, escape loss, and unseen Λ and K^0 decays. Threshold for ΞK production is 1.05 BeV/c, for $\Xi K\pi$ production, 1.38 BeV/c. Deuterium film was taken at 1.51 BeV/c only; the $\Xi^- K^0$ cross section was obtained by comparison of the corrected numbers of $\Xi^- K^0 p$ and $\Xi^- K^+ n$ events.

P_{beam} (BeV/c)	$\epsilon_{\text{c.m.}}$ (BeV)	$N/\mu\text{b}$	Ξ^- decays					Ξ^0 decays								
			$K^- p \rightarrow \Xi^- K^+$	$K^- p \rightarrow \Xi^- K^0 \pi^+$ (a)	$K^- p \rightarrow \Xi^- K^+ \pi^0$ (b)	$K^- d \rightarrow \Xi^- K^0 p$ (a)	$K^- p \rightarrow \Xi^- K^+ n$ (b)	$K^- p \rightarrow \Xi^- K^+ \pi N$ (c)	$K^- p \rightarrow \Xi^0 K^0$	$K^- p \rightarrow \Xi^0 K^0 \pi^0$ (a)	$K^- p \rightarrow \Xi^0 K^+ \pi^-$ (b)					
			N	σ (μb)	N_a	N_b	$\sigma_{\Xi^- K\pi}$ (μb)	N_a	N_b	N_c	N	σ (μb)	N_a	N_b	$\sigma_{\Xi^0 K\pi}$ (μb)	
1.05	1.815	0.26	0	≤ 7							2	46 \pm 35				
1.11											7	32 \pm 14				
1.22	1.896	1.19	33	49 \pm 9							10	42 \pm 19				
1.33	1.946	1.42	87	104 \pm 12							4	34 \pm 19				
1.43	1.991	0.795	75	159 \pm 20	0	0	≤ 2				4	34 \pm 19				
1.51	2.028	5.09	468	148 \pm 9	13	6	5.6 \pm 1.4	48	51	5	87	78 \pm 11	1	15	5.8 \pm 1.8	
1.60	2.066	0.715	60	133 \pm 18	11	4	32 \pm 8				13	91 \pm 28	3	10	48 \pm 17	
1.70	2.109	1.065	105	155 \pm 17	30	8	55 \pm 9				23	113 \pm 27	4	27	67 \pm 16	
Total:			828					104			146		8	52		
Grand total:					1004 Ξ^- decays							206 Ξ^0 decays				

II. DATA ANALYSIS

A determination of the lifetimes of the Ξ^- and Ξ^0 , based on essentially the same data sample, has been presented recently.² The selection criteria and kinematic analysis applied to individual events have been discussed there; highlights of the discussion are repeated here.

All film was double scanned according to a fixed set of scanning instructions for all events of the topologies of interest here. For acceptance, a candidate Ξ event was required to have a visible Λ decay; the $\Xi^0 K^0$ events were additionally required to have a visible K_1^0 decay. All candidates for cascade-hyperon productions were measured and analyzed. The measurements of each event were then constrained in the usual manner by the requirements of energy-momentum conservation.

In the case of the Ξ^- , the systematic biases in the sample were small. For example, the estimated loss rate for events with short Ξ^- 's is about 6% and for short Λ 's is about 2%. Further, we do not expect Λ -decay angular-distribution correlations with the Λ direction and the production normal for these missed events to be significantly biased. A similar loss of Ξ^0 's, estimated to be about 6%, occurs for events with short K_1^0 's. These loss mechanisms affect the angular distributions only through dependences on the laboratory momentum of the missed particles.

For Ξ^- events the distributions affected are the cascade production distribution $(d\sigma/d\Omega)_{\Xi}$ and the polarization intensity, $(Pd\sigma/d\Omega)_{\Xi}$. To minimize the systematic errors, a minimum acceptance length of 0.5 cm was imposed on both the Ξ^- and Λ for events used in fitting these distributions (Sec. III and IV). The accepted data were then weighted by a correction function of the form

$$Q(P_{\Xi}, P_{\Lambda}) = \exp \left[-\frac{0.5}{c} \left(\frac{M_{\Xi C}}{\tau_{\Xi} P_{\Xi}} + \frac{M_{\Lambda C}}{\tau_{\Lambda} P_{\Lambda}} \right) \right],$$

which depends only on the hyperon laboratory momenta. However, the cutoff events (some 11% of the data) were used in the analysis of the decay distributions described in Sec. V. A similar procedure was adopted for the $\Xi^0 K^0$ analysis to account for the short K^0 events.

Essentially no Ξ^- event of the topologies treated here was misidentified or confused with background from other reaction channels. For the Ξ^0 events, misinterpretation may furnish an additional source of systematic bias. The $\Xi^0 K^0$ events may be confused with topologically similar events produced by pion contamination in the beam; the $\pi^- p \rightarrow \Lambda K^0$ mode is essentially unambiguous, but the $\pi^- p \rightarrow \Sigma^0 K^0$ mode is kinematically similar to $K^- p \rightarrow \Xi^0 K^0$. Twenty-three events were ambiguous between $\Xi^0 K^0$ production and pion production modes. Twelve of these events gave a better fit to $\Xi^0 K^0$ production and are included in our sample. The consistency of the final apportionment was checked by comparing the number of events assigned to $\pi^- p \rightarrow \Sigma^0 K^0$ to the observed number of

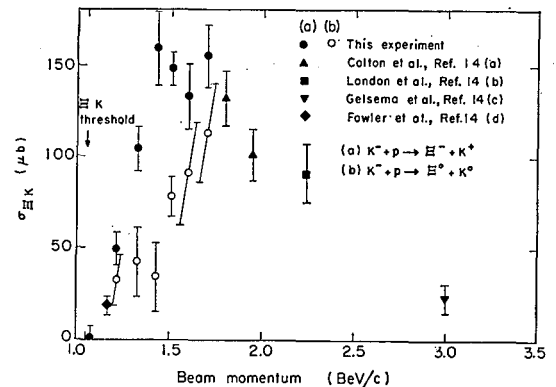


FIG. 1. Two-body production cross sections. As in Figs. 2, 5, and 6, the closed circles represent Ξ^- data, the open circles, Ξ^0 data. All cross sections are given in μb or $\mu\text{b}/\text{sr}$.

ΔK^0 events. We observe 39 ΔK^0 events and thus expect about 19 $\Sigma^0 K^0$ events. The final apportionment of 20 $\Sigma^0 K^0$ events (including unambiguous events) is consistent with this expectation.

The $\Xi^0 K^+ \pi^-$ events are topologically identical to much more copious production modes, such as $K^- p \rightarrow \Lambda \pi^+ \pi^-$. About 80% of the $\Xi^0 K^+ \pi^-$ events are kinematically unambiguous. Twenty-three candidate events were kinematically ambiguous; seven of these ambiguities were resolved by ionization. Our final sample of 52 $\Xi^0 K^+ \pi^-$ events includes six of the sixteen remaining ambiguous events; we estimate the contamination in the final sample to be about 3 events.

The $\Xi^0 K^0 \pi^0$ events are not kinematically overdetermined and have not been used in the decay analysis. The $(\Xi^0 \pi^0)$ mass has been determined by a missing-mass calculation utilizing the beam K^- and the K^0 . Ten events were consistent with $\Xi^0 K^0 \pi^0$ production. In six of the ten events, the fitted Λ was not consistent with coming directly from the production vertex; these events must be $\Xi^0 K^0 \pi^0$ events or the result of coincidences of unassociated V 's and normal K^0 events. The probable number of such coincidences is estimated to be less than one. Two of the four events in which the Λ is consistent with coming directly from the production vertex give acceptable fits to $\pi^- p \rightarrow \Delta K^0 \pi^0$. The remaining two events are ambiguous between $K^- p \rightarrow \Xi^0 K^0 \pi^0$ and $\pi^- p \rightarrow \Sigma^0 K^0 \pi^0$; we have included these as $\Xi^0 K^0 \pi^0$ events. The possibility of misinterpretation does not weaken our conclusions on the isotopic spin of the $\Xi^*(1530)$ presented in Sec. IV.

Deuterium data were obtained at 1.5 BeV/c, with

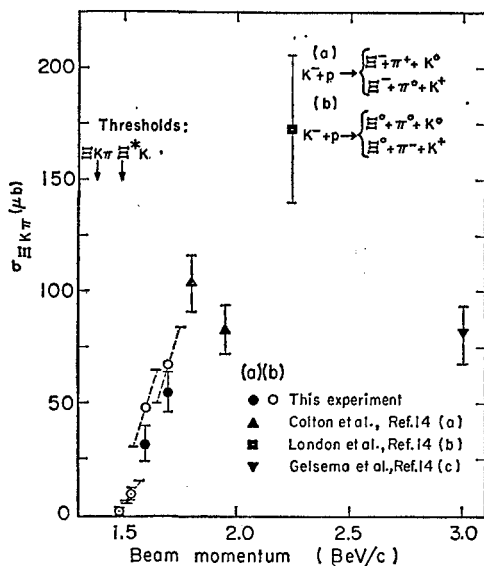


FIG. 2. Three-body production cross sections. The data from the 1.5-BeV/c exposure have been subdivided into low- and high-momentum subsamples (1.49 and 1.54 BeV/c) on the basis of the production fit. Path-length dependence on momentum was obtained from fitted data from other reaction channels, for which cross sections remain sensibly constant across the momentum range of the 1.5-BeV/c nominal beam setting.

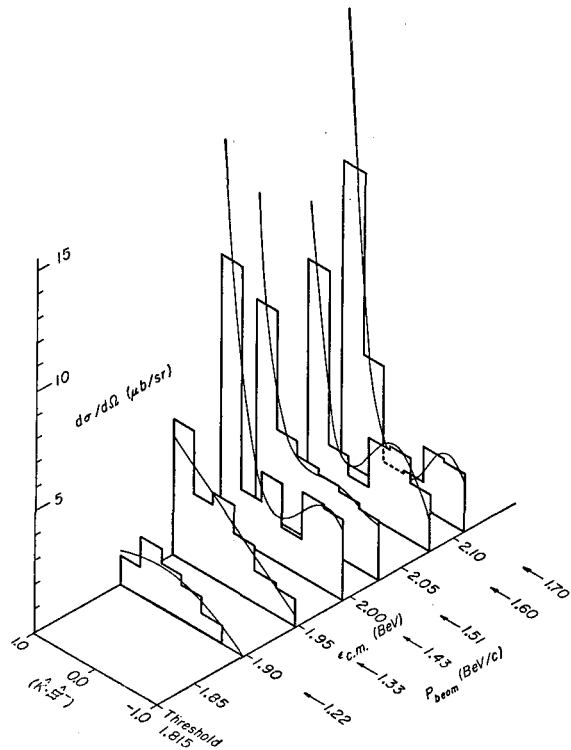


FIG. 3. $\Xi^- K^+$ differential cross sections at all momenta.

about 1/10 the path length of the corresponding hydrogen exposure. We feel few $\Xi^- K^+$ productions from protons were missed; the K^+ together with the Ξ^- and Λ decays provide a unique signature. On the other hand, $K^- n \rightarrow \Xi^- K^0$ events may be preferentially missed. For example, the interaction vertex of an event with an unseen spectator proton, no visible K^0 decay, and forward produced Ξ^- can be hard to determine; such events are almost surely counted as direct Λ productions. We compute a loss rate from this effect of about 6% (3 events). Even if the Ξ^- is not produced forward and the interaction vertex is known, the event may be misinterpreted; the interaction vertex cannot be constrained unless either the proton or the K_1^0 is observed. In accepting all such events as $\Xi^- K^0 p$, we may include as many as two $\Xi^- K^0 \pi^0 p$ events. (We actually saw one example of $\Xi^- K^0 \pi^0 p$, with both the K_1^0 decay and high-momentum spectator proton visible. This event was not included in the $\Xi^- K^0 p$ sample.) The free-nucleon cross sections presented have been further corrected to account for final-state ΞN interactions. Final-state ΞN interactions could be elastic, charge-exchange, pion-production, or double-hyperon-production—with or without extra pions. (KN interactions are negligible and have been duly neglected.) Elastic ΞN scatters do not change the number of events in the various channels, although they do distort the angular distributions. No example of double-hyperon production was observed. Two candidates for $\Xi N \rightarrow \Xi N \pi$ with high-momentum pro-

TABLE II. ΞK differential-cross-section expansion coefficients. The cross sections are represented by a Legendre polynomial expansion, $(d\sigma/d\Omega)_{\Xi K} = (\sigma/4\pi) \sum_{l=0}^L C_l P_l(\cos\theta_{\Xi})$, $C_0=1.0$. The Ξ^-K^0 data are the 40 "stationary" neutron events (proton recoil momentum less than 200 MeV/c). The error on C_0 is the cross-section fractional error of Table I.

P_{beam} (BeV/c)	Channel	$\sigma/4\pi$ (μb)	C_0	C_1	C_2	C_3	C_4
1.2	Ξ^-K^+	3.90	1.00 ± 0.18	0.78 ± 0.23	-0.66 ± 0.39	-0.66 ± 0.43	0.21 ± 0.57
1.3	Ξ^-K^+	8.28	1.00 ± 0.12	0.93 ± 0.14	-0.07 ± 0.26		
1.4	Ξ^-K^+	12.65	1.00 ± 0.13	0.80 ± 0.22	1.04 ± 0.26	0.96 ± 0.32	0.10 ± 0.42
1.5	Ξ^-K^+	11.78	1.00 ± 0.061	0.834 ± 0.082	0.733 ± 0.109	0.676 ± 0.128	0.164 ± 0.136
1.5	Ξ^0K^0	6.21	1.00 ± 0.14	0.79 ± 0.21	1.31 ± 0.20	-0.18 ± 0.29	
1.5	Ξ^-K^0	13.13	1.00 ± 0.21	0.65 ± 0.27	0.40 ± 0.36	0.59 ± 0.38	
1.6	Ξ^-K^+	10.58	1.00 ± 0.14	0.79 ± 0.24	0.96 ± 0.30	1.29 ± 0.30	0.62 ± 0.39
1.7	Ξ^-K^+	12.33	1.00 ± 0.11	1.29 ± 0.18	1.64 ± 0.19	1.23 ± 0.23	0.07 ± 0.24

tons were observed; of the five observed $\Xi^-K\pi N$ events, as many as four could be due to final-state pion production. Charge-exchange reactions are possible only between the neutral systems $\Xi^-p \leftrightarrow \Xi^0n$; from detailed balancing, the transition rates in either direction must be nearly equal. The net depopulation of Ξ^-K^0p events is then expected to be proportional to $\sigma_{\Xi^-K^0p} - \sigma_{\Xi^0K^0n}$, the difference in the production populations. We estimate a net decrease due to scanning losses and final-state interactions of $(17 \pm 7)\%$ for Ξ^-K^0p and $(7 \pm 5)\%$ for Ξ^-K^+n events. No attempt was made to analyze possible examples of Ξ^0 in the deuterium film.

The production angles for the deuterium events were calculated in the ΞK c.m. system. Only events with "spectator" nucleon momenta below 200 MeV/c in the laboratory system were included in the angular distributions. The validity of the impulse approximation was checked by comparing the differential cross section obtained from the 43 hydrogen-like Ξ^-K^+n events with that of the 468 hydrogen events at 1.5 BeV/c; these are found to be consistent. The data have been corrected as above for loss of short Ξ^- events, but no attempt has been made to adjust for distortions arising from misidentification of the produc-

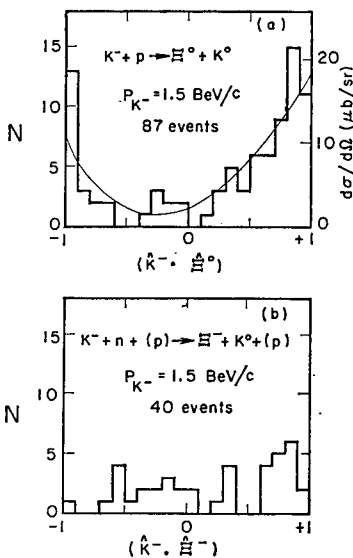


FIG. 4. ΞK differential cross sections at 1.5 BeV/c. (a) Ξ^0K^0 , (b) Ξ^-K^0 from the deuterium exposure at 1.5 BeV/c. Only the 40 stationary neutron events are included.

tion mode. The Ξ^-K^0 cross section was obtained by comparing the corrected numbers of Ξ^-K^0p and Ξ^-K^+n events and using the hydrogen value, $\sigma_{\Xi^-K^+} = 148 \pm 9 \mu\text{b}$.

Observed numbers of events, together with the corrected total cross sections in the various open reaction channels, are tabulated in Table I and displayed in Figs. 1 and 2.

III. ΞK PRODUCTION

Cross sections and polarizations for two-body Ξ production are displayed in Figs. 1 and 3 to 7.⁶ Combining our hydrogen and deuterium results for the Ξ^-K^+ , Ξ^0K^0 , and Ξ^-K^0 production processes, we compute the production rates for ΞK in $I=0$ and $I=1$,

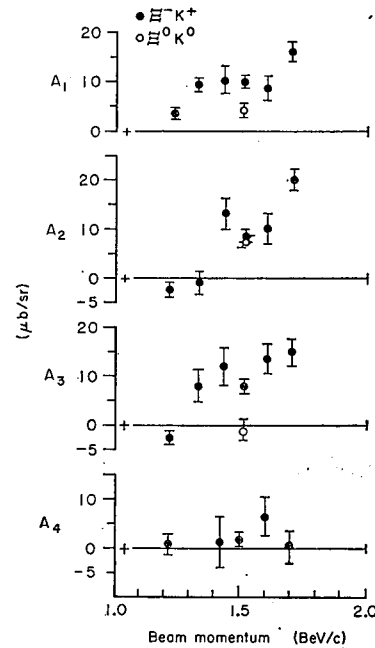


FIG. 5. ΞK differential-cross-section Legendre-polynomial expansion coefficients. The zeroth-order term is $A_0 = \sigma/4\pi$.

⁶ The polarization points and errors are essentially those obtained in Sec. V by fitting the distribution function (5.11) to the data. The errors include the statistical effect of possible variation in the decay parameters. The decay parameters used for the Ξ^- are those of Table V, column 2; for the Ξ^0 , those of column 5. If the decay parameters given in column 6 (resulting from the assumptions $\alpha_{\Xi^-} = \alpha_{\Xi^0}$, $\Phi_{\Xi^-} = \Phi_{\Xi^0}$) are used, $\langle P_{\Xi^0} \rangle = -0.52 \pm 0.20$ in our energy region.

TABLE III. $\Xi\pi K$ cross sections. Total $\Xi\pi K$ cross sections for all charge combinations are given in columns 4 through 7. Estimated numbers of $\Xi^*(1530)$ events above background and Ξ^*K cross sections are given in columns 8 and 9.

P_{beam} (BeV/c)	$\epsilon_{\text{c.m.}}$ (BeV)	$N/\mu\text{b}$	$\Xi^-\pi^+K^0$		$\Xi^0\pi^0K^0$		$\Xi^0\pi^-K^+$		$\Xi^-\pi^0K^+$		$\Xi^*(1530)$ production			
			N	σ	N	σ	N	σ	N	σ	N	σ	N	σ
1.49	2.019	2.545	3	1.8 ± 1.0	0	≤ 2	4	2.5 ± 1.5	0	≤ 0.6	0	≤ 0.7	4	2.5 ± 1.5
1.54	2.041	2.545	10	5.9 ± 1.9	1	2.2 ± 2.2	11	6.9 ± 2.4	6	3.4 ± 1.4	10	8 ± 3	15	9 ± 3
1.60	2.066	0.715	11	24 ± 7	3	23 ± 14	10	25 ± 9	4	8 ± 4	12	35 ± 11	12	28 ± 9
1.70	2.109	1.065	30	44 ± 8	4	22 ± 13	27	45 ± 11	8	11 ± 4	31	61 ± 12	26	41 ± 10
Total			54		8		52		18		53		57	

and the phase difference δ of the I -spin production amplitudes at 1.51 BeV/c. We obtain

$$\begin{aligned} \sigma(\Xi^-K^+) &= 148 \pm 9 \mu\text{b} = |(a_0 + a_1)/2|^2; & \sigma_0 &= 287 \pm 44 \mu\text{b} \\ \sigma(\Xi^0K^0) &= 78 \pm 11 \mu\text{b} = |(a_0 - a_1)/2|^2; & \sigma_1 &= 165 \pm 34 \mu\text{b} \\ \sigma(\Xi^-K^0) &= 165 \pm 34 \mu\text{b} = |a_1|^2; & \delta &= 71 \pm 4 \text{ deg.} \end{aligned}$$

At 1.51-BeV/c incident-beam K^- momentum, the invariant mass of the $S=-1$, $B=1(K^-p)$ system is 2.026 BeV, corresponding closely to the predicted position of the first Regge recurrences of either the $Y_1^*(1385)$ or the $Y_0^*(1405)$ [we assume $J^P = \frac{1}{2}^-$ for $Y_0^*(1405)$].⁷ We might then hope to observe resonant enhancement of either the $I=1$, $F_{7/2}$ or $I=0$, $D_{5/2}$ amplitudes in such systems at 1.51 BeV/c. The ΞK system is particularly suitable for such an investigation; the high-quality polarization information available through observation of both the Ξ and Λ decay together with the observed production distribution $d\sigma/d\Omega$ allow in principle a complete partial-wave analysis.

As a first step, the differential-cross-section data for Ξ^0K^0 and Ξ^-K^0 at 1.5 BeV/c and the Ξ^-K^+ at all momenta were fitted with a Legendre-polynomial expansion to determine the maximum complexity; the resulting fit coefficients are displayed in Table II and in Fig. 5. We find that the data nowhere require more

than third order to give an acceptable fit; at 1.5 BeV/c, the Ξ^-K^0 data from deuterium are well fitted with first order, while the Ξ^0K^0 require second order. For the Ξ^-K^+ channel, 1.2 and 1.3 BeV/c are adequately fitted with first order; above 1.3 BeV/c, the data require up to third order (the requirement at 1.4 BeV/c is somewhat marginal, corresponding to about 2.5 standard deviations). The only region with possibly rapidly varying production amplitudes is between 1.3 and 1.4 BeV/c, where our data are extremely limited. To include the polarization information, a maximum-likelihood partial-wave fit of the Ξ^-K^+ data at each momentum was performed; this fit (rather than the polynomial-expansion fit), yielded the curves of Figs. 3, 4, and 7 (no attempt was made to include possible energy dependence of the partial-wave parameters). The fitted polarizations are shown in Figs. 6 and 7. We found that inclusion of states only up through $L=2$ yields an adequate fit at 1.5 BeV/c. The data nowhere require more than D waves. We conclude that we have no significant evidence for possible resonant behavior in the ΞK channel below 1.7 BeV/c.

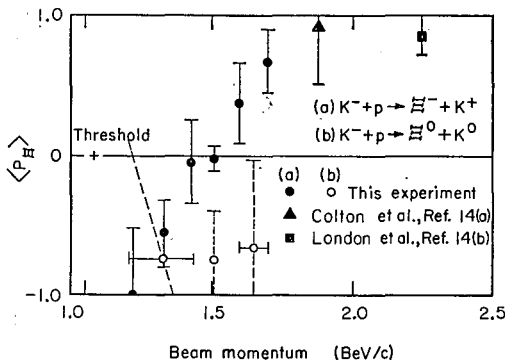


Fig. 6. ΞK polarization. The average polarization projection along the production normal $\hat{n} = (\hat{K}^- \times \hat{\Xi}) / |\hat{K}^- \times \hat{\Xi}|$ at each momentum was estimated from the distribution function (5.11).

⁷ R. L. Schult and R. H. Capps, Nuovo Cimento 23, 416 (1962).

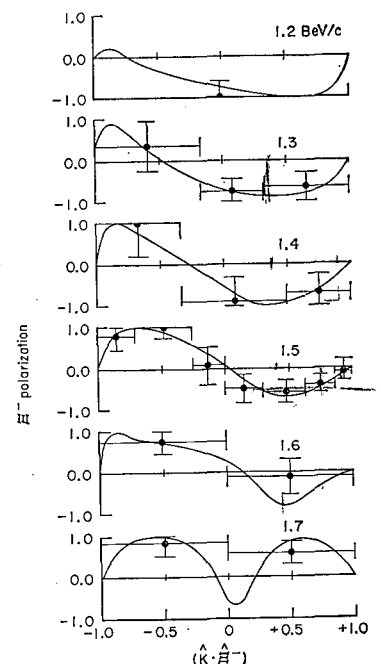


Fig. 7. Ξ^-K^+ polarization dependence on production angle. The smooth curves result from the same partial-wave fit to the data that gave the smooth curves of Fig. 3. The data points were calculated as described in Ref. 6. The sign convention is the same as in Fig. 6.

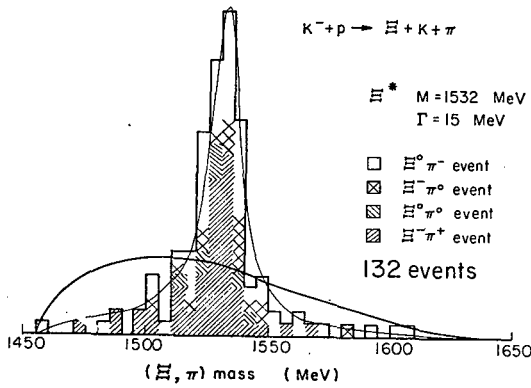


FIG. 8. $(\Xi\pi)$ mass distribution. There are 132 examples of $\Xi K\pi$ production, plotted in the mass histogram. The two smooth curves correspond to pure phase space, and to an incoherent mixture of 20% phase space, 80% Ξ^* production.

IV. $\Xi\pi K$ PRODUCTION

Production cross sections for the three-body $\Xi\pi K$ final state in our momentum region are shown in Table III and Fig. 2. The prominent features in this channel are the similarity of the $\Xi^-\pi K$ and $\Xi^0\pi K$ cross sections, and the predominance of $\Xi^*(1530)$ formation.

Production of a pure $\Xi\pi$ resonance in either possible isospin state can be shown to yield equal $\Xi^-\pi K$ and $\Xi^0\pi K$ production rates, provided that there is no interference between production states or if one production state dominates. Deuterium data might then be used to attempt to identify these production states; our data are unfortunately too limited to serve this purpose.

The formation of $\Xi^*(1530)$ accounts for most of the three-body production data, even at threshold. The $(\Xi\pi)$ mass distribution (Fig. 8) is acceptably reproduced by an incoherent mixture of $\frac{1}{5}$ nonresonant $\Xi\pi K$ and $\frac{4}{5}$ Ξ^*K production, with a resonant mass of 1532 MeV and a width of 15 MeV. The experimental mass-resolution function yields a full width of about 6 MeV for $\Xi^-\pi^+$ and $\Xi^-\pi^0$, 9 MeV for $\Xi^0\pi^-$, and more than 15 MeV for $\Xi^0\pi^0$ events. Taking only the 54 $\Xi^-\pi^+$ events to avoid mass-difference effects,⁸ we obtain an experimental width of 9 ± 3 MeV, and thus a true resonant width of about 7 ± 7 MeV. This value is consistent with earlier results.^{9,10}

The total cross section obtained for Ξ^* production is

⁸ (a) G. M. Pjerrou, P. E. Schlein, W. E. Slater, L. T. Smith, D. H. Stork, and H. K. Ticho, *Phys. Rev. Letters* **14**, 275 (1965); (b) G. W. London, R. R. Rau, N. P. Samios, S. S. Yamamoto, M. Goldberg, S. Lichtman, M. Primer, and J. Leitner, *Phys. Rev.* **143**, 1034 (1966).

⁹ L. Bertanza, V. Brisson, P. L. Connolly, E. L. Hart, I. S. Mitra, G. C. Moneti, R. R. Rau, N. P. Samios, I. O. Skillicorn, S. S. Yamamoto, M. Goldberg, L. Gray, J. Leitner, S. Lichtman, and J. Westgard, *Phys. Rev. Letters* **9**, 180 (1962).

¹⁰ P. E. Schlein, D. D. Carmony, G. J. Pjerrou, W. E. Slater, D. H. Stork, and H. K. Ticho, *Phys. Rev. Letters* **11**, 167 (1963); G. M. Pjerrou, D. J. Prowse, P. Schlein, W. E. Slater, D. H. Stork, and H. K. Ticho, *ibid.* **9**, 114 (1962); J. Button-Shafer, J. S. Lindsey, J. J. Murray, and G. A. Smith, *Phys. Rev.* **142**, 883 (1966).

shown in Fig. 9. (We have split the data from the 1.5 BeV/c nominal beam setting into high- and low-momentum sections to show the very sharp rise in the excitation function near threshold more clearly.) The relative abundance of the four charge combinations in the Ξ^* peak confirms earlier results leading to the assignment $I=\frac{1}{2}$ for this resonance.^{9,10} The production and decay of an $I=\frac{3}{2}$ Ξ^* requires $(\Xi^-\pi^+):(\Xi^0\pi^0):(\Xi^0\pi^-):(\Xi^-\pi^0)=1:2:1:2$; $I=\frac{1}{2}$ requires $(\Xi^-\pi^+):(\Xi^0\pi^0)=(\Xi^0\pi^-):(\Xi^-\pi^0)=2:1$ (any ratio of Ξ^{*0} to Ξ^{*-} is allowed). Taking all events from all momenta with $(\Xi\pi)$ mass between 1510 and 1550 MeV, we obtain

$$(\Xi^-\pi^+):(\Xi^0\pi^0):(\Xi^0\pi^-):(\Xi^-\pi^0)=45:(3 \times 8=24):39:16$$

(the $\Xi^0\pi^0$ data was corrected for the probability of charged K_1^0 decay). These results are seen to be in excellent agreement with the $I=\frac{1}{2}$ assignment for the $\Xi^*(1530)$; they are completely inconsistent with $I=\frac{3}{2}$. Estimated Ξ^*K cross sections are given in Table III; the $I=\frac{1}{2}$ assignment for the Ξ^* was used explicitly in correcting for unseen decays.

The Ξ^* production and decay angular distributions are displayed in Fig. 10; all events with $(\Xi\pi)$ mass between 1.51 and 1.55 BeV are included. At threshold, the Ξ^*K system might be expected to be in an S -wave orbital state; the production distribution near 1.51 BeV/c is consistent with isotropy, and thus with S -wave production, with a 50% confidence level. Then Ξ^* events at all production angles may be treated in the manner first proposed by Adair.¹¹ The fits of the decay cosine $(\hat{K} \cdot \hat{\Xi})$ yield a 12% confidence level for isotropy.

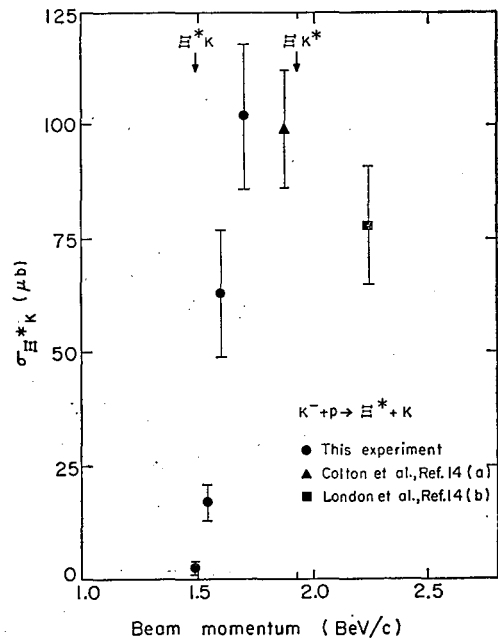


FIG. 9. Ξ^* production cross section. The sum of the $\Xi^{*-}K^+$ and $\Xi^{*0}K^0$ cross sections is given.

¹¹ Robert K. Adair, *Phys. Rev.* **100**, 1540 (1955).

and a 99% confidence level for the fit to $[1+3(\hat{K} \cdot \hat{\Xi})^2]$. This result is consistent with the results of Schlein *et al.*,¹⁰ $J_{\Xi^*} \geq \frac{3}{2}$, but is not by itself sufficient evidence to rule out $J_{\Xi^*} = \frac{1}{2}$.

V. ANALYSIS OF NONLEPTONIC DECAYS

A. General Discussion

A collection of particles with spin J can be completely described in their rest frame by the expectation values of spin operators, the number and dimensionality of which are determined by the spin of the particles. Knowledge of these expectation values is equivalent to knowledge of the probability amplitudes for occupation of the various (J, M) quantum-mechanical states permitted for the particles. If the particles are unstable, the character of their original state and the transition amplitudes for decay completely determine the angular dependence of directions and polarizations of final-state particles.

In the particular case of nonleptonic decay of the Ξ hyperon with spin J into a spinless pion and a spin- $\frac{1}{2}$ Λ , two orbital angular momenta are possible, with amplitudes $A_l = A_{J-1/2}$ and $A_{J+1/2}$. We define the real decay parameters as¹²⁻¹⁴

$$\begin{aligned} \alpha_{\Xi} &= 2 \operatorname{Re}(A_{J-1/2}^* A_{J+1/2}) / \lambda_{\Xi} = (2 |A_{J-1/2}| |A_{J+1/2}| / \lambda_{\Xi}) \\ &\quad \times \cos(\delta_+ - \delta_-) \\ \beta_{\Xi} &= 2 \operatorname{Im}(A_{J-1/2}^* A_{J+1/2}) / \lambda_{\Xi} = (2 |A_{J-1/2}| |A_{J+1/2}| / \lambda_{\Xi}) \\ &\quad \times \sin(\delta_+ - \delta_-) = (1 - \alpha_{\Xi}^2)^{1/2} \sin \Phi_{\Xi} \\ \gamma_{\Xi} &= (|A_{J-1/2}|^2 - |A_{J+1/2}|^2) / \lambda_{\Xi} = (1 - \alpha_{\Xi}^2)^{1/2} \cos \Phi_{\Xi}, \end{aligned} \quad (5.1)$$

where $\lambda_{\Xi} = (|A_{J-1/2}|^2 + |A_{J+1/2}|^2)$. [Expression of the unit vector $(\alpha, \beta, \gamma)_{\Xi}$ in terms of the spherical coordinates α_{Ξ} and $\Phi_{\Xi} = \tan^{-1}(\beta/\gamma)_{\Xi}$ has the advantage of yielding a description of the decay amplitudes in terms of parameters that are experimentally found to be nearly uncorrelated.] Imposition of parity conservation in the Ξ decay would require one of the two decay amplitudes to vanish; existence of a nonzero α_{Ξ} or β_{Ξ} therefore implies parity nonconservation in this process. The angle $(\delta_+ - \delta_-)$ defined above is the phase difference between the two observed decay amplitudes and includes a contribution both from the original amplitudes and from the interaction in the final state of the $\Delta\pi$

¹² W. B. Teutsch, S. Okubo, and E. C. G. Sudarshan, *Phys. Rev.* **114**, 1148 (1959); T. D. Lee, J. Steinberger, G. Feinberg, P. K. Kabir, and C. N. Yang, *ibid.* **106**, 1367 (1957).

¹³ N. Byers and S. Fcnster, *Phys. Rev. Letters* **11**, 52 (1963).

¹⁴ (a) E. Colton, P. Dauber, W. Dunwoodie, G. M. Pjerrou, P. Schlein, W. E. Slater, L. Smith, D. H. Stork, and H. K. Ticho, (to be published). (b) London *et al.*, *Ref.* 8(b). (c) E. S. Gelsema, J. C. Kluyver, A. G. Tenner, M. Demoulin, J. Goldberg, B. P. Gregory, G. Kayas, P. Krejbich, C. Pelletier, M. Ville, R. Barloutaud, A. Leveque, C. Louedec, J. Meyer, and A. Verglas, in *Proceedings of the Sienna International Conference on Elementary Particles, 1963* (Società Italiana di Fisica, Bologna, Italy, 1963), Vol. I, p. 143. (d) W. B. Fowler, R. W. Birge, P. Eberhard, R. P. Ely, M. L. Good, W. M. Powell, and H. K. Ticho, *Phys. Rev. Letters* **6**, 134 (1961); the detector in this last experiment was a propane bubble chamber.

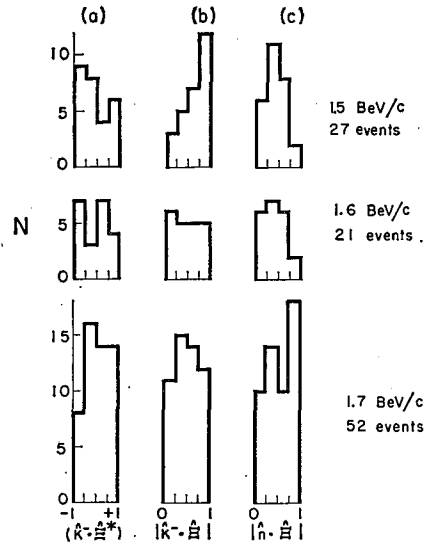


FIG. 10. Ξ^* production and decay angular distributions. (a) Ξ^* production distribution, (b) Ξ^* decay alignment with the beam direction ("Adair" angle), folded about $(\hat{K} \cdot \hat{\Xi}) = 0$; and (c) Ξ^* decay alignment with the production normal, folded about $(\hat{n} \cdot \hat{\Xi}) = 0$.

system at an invariant mass equal to the Ξ^* mass. Imposition of time-reversal invariance on the decay transition would require these original decay amplitudes to be relatively real, giving a contribution of zero or π to $(\delta_+ - \delta_-)$. Charge-conjugation invariance would require these amplitudes to be relatively imaginary, giving a contribution of $\pm\pi/2$.

A value for λ_{Ξ} , the decay rate, was presented in *Ref.* 2. Here we analyze the data in an attempt to obtain $(J, \alpha, \Phi)_{\Xi}$.

Observed angular distributions are customarily fit with cosine series or with series of Legendre polynomials: the latter have the advantage of being orthogonal functions so that the addition of higher order polynomials in fitting data does not appreciably change lower order coefficients. Dependence on azimuthal angle in addition to polar angle is manifested in decays of particles having spin higher than $\frac{1}{2}$; thus the spherical harmonics $Y_{LM}(\theta, \phi)$ or the symmetrical-top functions $\mathcal{D}_{MM}^J(\phi, \theta, 0)$ rather than Legendre polynomials $P_L(\theta)$, are convenient for fitting the complete decay distributions.¹⁵

Testing data for compatibility with various spin hypotheses is possible through the determination of the highest order spherical harmonics needed to fit the decay distributions, since the maximum L value of the Y_{LM} required is the maximum rank of spin operator needed to describe the original set of particles. The spin J is related to the maximum permissible

¹⁵ The functions \mathcal{D}_{MM}^L may be decomposed into sums of spherical harmonics. See, for example, M. Jacob and G. C. Wick, *Ann. Phys.* **7**, 404 (1959), or A. R. Edmonds, *Angular Momentum in Quantum Mechanics* (Princeton University Press, Princeton, New Jersey, 1957).

rank (L) through the requirement that $L_{\max}=2J$. It is generally impossible to say whether there has been some fortuitous cancellation of high- L terms; hence the complexity of the decay distributions places only a lower limit on J .

The polarization parameters of the initial state and the decay amplitudes are overdetermined by the complete angular and polarization distributions of the final decay fermion. If available data have statistically significant polarization parameters, consistency checks may be made on the data under various spin hypotheses.

B. Formalism

A convenient formalism for this analysis is that developed by Byers and Fenster.¹³ Their treatment, utilizing irreducible tensors as spin operators, represents the Ξ initial state by a density matrix of the form

$$\rho = (2J+1)^{-1} \sum_{L=0}^{2J} \sum_{M=-L}^L (2L+1) \langle T_{LM} \rangle^* T_{LM} \quad (5.2)$$

for any (half-integral) spin J . Here the T_{LM} are spin-space operators which may be constructed from the operators S_x , S_y , and S_z in a manner similar to the construction of the spherical harmonics Y_{LM} from the coordinates x , y , and z . (The analogy is not exact because of the difference in commutation properties.)

With the production normal $\hat{n} = (\hat{K}^- \times \hat{\Xi}) / |\hat{K}^- \times \hat{\Xi}|$ as the z axis and the incident K^- direction as the y axis, the polar angles θ and ϕ characterize the Λ direction in the Ξ rest frame. To describe the polarization components of the Λ , we choose for a coordinate system the triad $(\hat{x}, \hat{y}, \hat{\Lambda})$, where $\hat{\Lambda}$ is a unit vector along the Λ flight path in the Ξ rest frame, and $\hat{x} = \hat{\Lambda} \times (\hat{\Lambda} \times \hat{n}) / |\hat{\Lambda} \times \hat{n}|$ and $\hat{y} = (\hat{n} \times \hat{\Lambda}) / |\hat{\Lambda} \times \hat{n}|$ are evaluated in the Λ rest frame.

Defining for convenience E_L and O_L as 1 (0) and 0 (1) if L is even (odd), and abbreviating $\langle T_{LM} \rangle$ as t_{LM} , we write the Λ angular distribution and polarization components in terms of the density matrix elements:

$$I_{\Lambda}(\theta, \phi) = \sum_{L=0}^{2J} \sum_{M=-L}^L (E_L + \alpha_{\Xi} O_L) (n_{L0}^J t_{LM}) \times Y_{LM}^*(\theta, \phi), \quad (5.3a)$$

$$I_{\Lambda} \mathbf{P}_{\Lambda} \cdot \hat{\Lambda} = \sum_{L=0}^{2J} \sum_{M=-L}^L (\alpha_{\Xi} E_L + O_L) (n_{L0}^J t_{LM}) \times Y_{LM}^*(\theta, \phi), \quad (5.3b)$$

$$I_{\Lambda} \mathbf{P}_{\Lambda} \cdot (\hat{x} + i\hat{y}) = (i\beta_{\Xi} - \gamma_{\Xi}) \sum_{L=0}^{2J} \sum_{M=-L}^L O_L \left(\frac{2L+1}{4\pi} \right)^{1/2} \times (n_{L1}^J t_{LM}) \mathfrak{D}_{M1}^L(\phi, \theta, 0), \quad (5.3c)$$

$$I_{\Lambda} \mathbf{P}_{\Lambda} \cdot (\hat{x} + i\hat{y}) = (2J+1) (i\beta_{\Xi} - \gamma_{\Xi}) (4\pi)^{-1/2} \times \sum_{L=0}^{2J} \sum_{M=-L}^L O_L \left(\frac{2L+1}{L(L+1)} \right)^{1/2} (n_{L0}^J t_{LM}) \times \mathfrak{D}_{M1}^L(\phi, \theta, 0). \quad (5.3d)$$

The n_{L0}^J and n_{L1}^J are quantities proportional to Clebsch-Gordan coefficients, needed to modify the single spherical harmonics resulting from the combination of the two decay amplitudes¹⁶;

$$n_{L0}^J = (-1)^{J-1/2} \left(\frac{2J+1}{4\pi} \right)^{1/2} C(JJL; \frac{1}{2}, -\frac{1}{2}) \quad (5.4a)$$

and

$$n_{L1}^J = (-1)^{J-1/2} \left(\frac{2J+1}{4\pi} \right)^{1/2} C(JJL; \frac{1}{2}, \frac{1}{2}) = O_L (2J+1) [L(L+1)]^{-1/2} n_{L0}^J. \quad (5.4b)$$

Equation (5.3d) follows from (5.3c) by use of (5.4b), and displays explicitly the J_{Ξ} dependence of the Λ transverse polarization. The requirement of parity conservation in the strong production process imposes the condition that the odd- M terms in (5.3) vanish when \hat{n} is chosen as the axis of quantization.

The terms containing t_{00} may be extracted from (5.3) and combined to give the well-known result that, independent of Ξ spin or polarization, when averaged over Ξ decay directions, the Λ decay distribution along the Λ line of flight is just $1 + \alpha_{\Lambda} \alpha_{\Xi} (\hat{\Lambda} \cdot \hat{\phi})$, where $\hat{\phi}$ is a unit vector along the proton direction in the Λ rest frame.¹⁷ The coefficients of the odd- L terms in (5.3) yield information on $\Phi_{\Xi} = \tan^{-1}(\beta/\gamma)_{\Xi}$, J , and the magnitudes of α_{Λ} and α_{Ξ} .

Determination of the spin factor $(2J+1)$ was attempted via two different statistical approaches. The first of these, called the "ratio test," was suggested by Ademollo and Gatto¹⁸ and by Byers and Fenster. It uses the orthogonality properties of the Y_{LM} and \mathfrak{D}_{M1}^L to project out "moments" (i.e., coefficients of the Y_{LM}^* and the \mathfrak{D}_{M1}^L) from the experimental distributions. The moments corresponding to some odd L may then be combined to give a direct experimental measure of the spin.

Alternatively, one may utilize the redundancy in the determinations of the moments to calculate test functions on the consistency of the data with particular spin assumptions. For this second statistical approach we adopted a maximum-likelihood method. Here we attempted to distinguish between spins $\frac{1}{2}$ and $\frac{3}{2}$ on the basis of the resultant values of the normalized likelihoods.

C. Moment Analysis and the Ratio Test

As remarked above, the orthogonality properties of the expansion polynomials Y_{LM} and \mathfrak{D}_{M1}^L allow the projection [for each (L, M) value] of the expansion coefficients from the distributions (5.3). Then, for

¹⁶ The notation is $C(j_1, j_2, J; m_1, m_2)$, where $j_1 + j_2 = J$.

¹⁷ We may fit our Ξ decay data with this spin-independent distribution function. We find $(\alpha_{\Lambda} \alpha_{\Xi}) = -0.245 \pm 0.046$, and $(\alpha_{\Lambda} \alpha_{\Xi}^0) = -0.18 \pm 0.14$. These results are consistent with the world compilation in Ref. 19.

¹⁸ M. Ademollo and R. Gatto, Nuovo Cimento 30, 429 (1963).

some value of (L, M) , with index k running over events, we obtain the equations

$$(E_L + \alpha_{\Xi} O_L)(n_{L0}^J t_{LM}) = \int_{\Omega} Y_{LM}(\theta, \phi) I_{\Lambda}(\theta, \phi) d\Omega$$

$$= \langle Y_{LM} \rangle \sim \left(\frac{1}{N} \sum_{k=1}^N Y_{LM}(\theta_k, \phi_k) \right), \quad (5.5a)$$

$$(O_L + \alpha_{\Xi} E_L)(n_{L0}^J t_{LM}) = \langle Y_{LM} \mathbf{P}_{\Lambda} \cdot \hat{\Lambda} \rangle$$

$$\sim \left(\frac{1}{N} \sum_{k=1}^N Y_{LM}(\theta_k, \phi_k) (\hat{\Lambda} \cdot \hat{p})_k \right), \quad (5.5b)$$

and

$$O_L(2J+1)(i\beta_{\Xi} - \gamma_{\Xi})(n_{L0}^J t_{LM}) \sim \left[\frac{L(L+1)(2L+1)^{-1/2}}{4\pi} \right]$$

$$\times \left(\frac{1}{N} \sum_{k=1}^N \mathfrak{D}_{M1}^{L*}(\phi_k, \theta_k, 0) (\hat{x} \cdot \hat{p} + i\hat{y} \cdot \hat{p})_k \right). \quad (5.5c)$$

Real and imaginary parts of the moments may be found from (5.5c) through use of the symmetry relation $t_{LM} = (-1)^M t_{LM}^*$. The existence of any of the moments (5.5) with $L > 1$ would serve to demonstrate $J > \frac{1}{2}$. We found no significant (i.e., more than 2.5 standard deviations from zero) higher order moment in any subsample of our data.

The separate projections of the coefficients permit evaluation, for any (odd- L, M) combination, of

$$(2J+1)^2$$

$$= \frac{[\beta_{\Xi}(2J+1)(n_{L0}^J t_{LM})]^2 + [\gamma_{\Xi}(2J+1)(n_{L0}^J t_{LM})]^2}{[(n_{L0}^J t_{LM})]^2 - [\alpha_{\Xi}(n_{L0}^J t_{LM})]^2}. \quad (5.6)$$

Equation (5.6) is obtained with the help of the constraint equation $\alpha_{\Xi}^2 + \beta_{\Xi}^2 + \gamma_{\Xi}^2 = 1$. Meaningful estimation of $(2J+1)^2$ from (5.6) requires data characterized by some nonzero, odd- L moment t_{LM} . Since the higher ($L > 1$) moments were experimentally found to vanish, and as t_{10} is the only moment that can in principle exist for all spins, we sought to evaluate (5.6) for $L=1$. (Note that, for spin- $\frac{1}{2}$, the average sample polarization P_{Ξ} is $\sqrt{3}t_{10}$.)

The average polarization of the total data was found to be very small (see Fig. 6); thus the data were partitioned according to production energy and production angle into subsamples, some of which were found to have $t_{10} \neq 0$ (see Fig. 7). Available statistical precision was such that no one of the subsamples yielded a definitive spin determination. An estimate of the t_{10} value for each of these subsamples was formed by averaging the experimental sample moments t_{10} , samples to rotate depends on the sign of the experimental $(\alpha_{\Xi} t_{10})/\alpha_w$, and $(\gamma_{\Xi} t_{10})/\gamma_w$. [The numerators represent terms from the (1,0) moments of Eqs. (5.5), while $\alpha_w = -0.48$ and $\gamma_w = 0.85$ are the world-average values

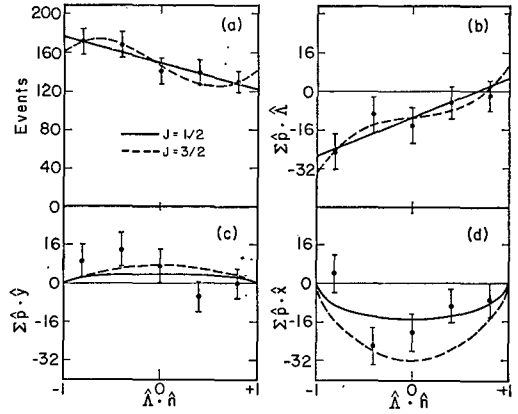


FIG. 11. Intensity and polarization-component distributions for the combination of the four data samples discussed in Sec. IVC. Figure 11, (a) through (d), represents the distributions I_{Λ} , $\alpha_{\Lambda}(\mathbf{P}_{\Lambda} \cdot \hat{\Lambda})/3$, $\alpha_{\Lambda}(\mathbf{P}_{\Lambda} \cdot \hat{y})/3$, and $\alpha_{\Lambda}(\mathbf{P}_{\Lambda} \cdot \hat{x})/3$ as functions of the decay cosine $(\hat{\Lambda} \cdot \hat{n})$ [see Eq. (5.5)]. Moments projected from distributions (a) and (b) were used to calculate the curves shown on all four plots (the solid lines arise from the assumption $J = \frac{1}{2}$; the dashed, from $J = \frac{3}{2}$). Moments obtained from distributions (c) and (d) give curves similar to and consistent with the solid curves shown.

of the Ξ^- decay parameters available at the time of the analysis.¹⁹

For this analysis, the data were subdivided into four momentum-angle samples. Each sample was characterized by having t_{10} differing from zero by at least two standard deviations. The four samples were (A) data from 1.2 through 1.4 BeV/c, t_{10} (estimated as above) $= -0.29 \pm 0.10$; (B) 1.5-BeV/c forward production, $t_{10} = -0.20 \pm 0.09$; (C) 1.5-BeV/c backward production, $t_{10} = 0.40 \pm 0.11$; and (D) 1.6 and 1.7 BeV/c, $t_{10} = 0.23 \pm 0.12$. The four $\beta_{\Xi} t_{10}$ moments were found to be very small, consistent with the predictions of time-reversal invariance.

Expression (5.6) was evaluated for each of the four subsamples through use of the four (1,0) moments. Additional accuracy was obtained by recasting the denominator term into the form $(1 - \alpha_w^2)(n_{L0}^J t_{L0})^2$ and estimating $(n_{10}^J t_{10})$ from the weighted average of $(n_{10}^J t_{10})$ and $(n_{10}^J \alpha_{\Xi} t_{10})/\alpha_w$. The data from negative-polarization samples can be combined with those from positive-polarization samples by rotating the coordinate system used in the decay analysis of the former by 180 deg about the incident K^- direction [only the sign of t_{10} in Eqs. (5.5) is changed by this rotation]. Our estimate of the spin factor $2J+1$ from the combined sample ranges from 2.86 to 2.18 as α_{Ξ} varies from -0.48 (the "world-average" result) to -0.34 (the value obtained from the t_{00} moment of our data). Estimates of $2J+1$ made by omitting the $\beta_{\Xi} t_{10}$ moment (equivalent to the physical assumption $\beta_{\Xi} = 0$) are smaller by about 1%. The choice of which

¹⁹ Harold K. Ticho, in *Proceedings of the International Conference on Fundamental Aspects of Weak Interactions, 1963* (Brookhaven National Laboratory, Upton, New York, 1963), p. 4.0.

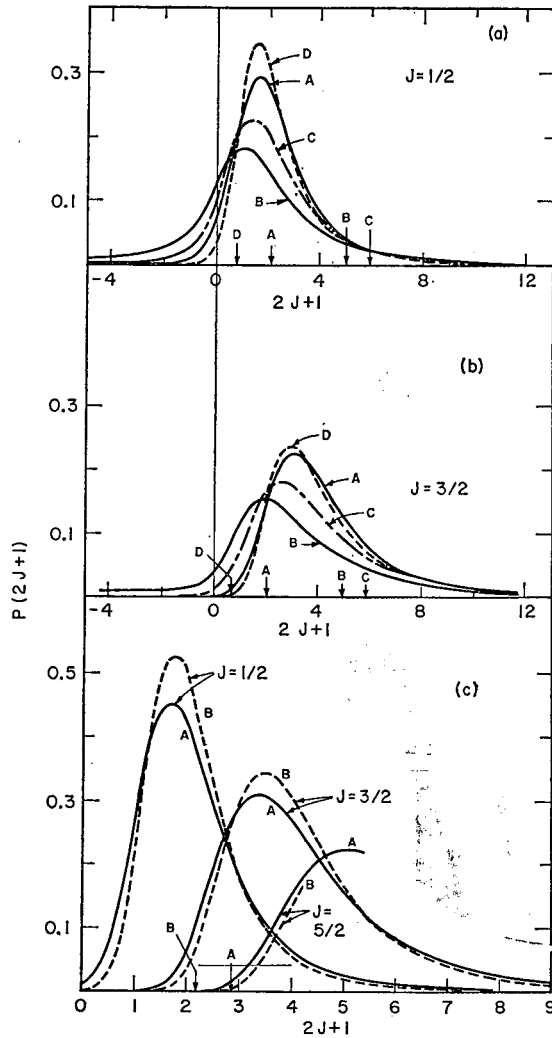


FIG. 12. (a) Evaluations (arrows) and probability distributions of $(2J+1)$ for four simply selected data samples: (A) 1.2 through 1.4 BeV/c; (B) 1.5 BeV/c, forward production; (C) 1.5 BeV/c, backward production; and (D) 1.6 through 1.7 BeV/c. A true spin of $\frac{1}{2}$ is assumed for the calculated distributions. (b) Data used are the same as for (a). Spin $\frac{3}{2}$ is assumed for probability distributions. (c) Evaluation and probability distributions of $(2J+1)$ from the total data, treated as a combination of the four samples used for (a) and (b) (see text). Spins $\frac{1}{2}$, $\frac{3}{2}$, and $\frac{5}{2}$ are assumed for the probability distributions. All curves are normalized to have the same area. Here the arrows and curves are designated by A for $\alpha_z = -0.48$ and by B for $\alpha_z = -0.34$.

mentally determined moments; this dependence may yield a biased result. Since these signs were in each case determined by at least two standard deviations, we believe this effect to be small.

Figure 11 presents histograms of the Λ intensity and polarization distributions as functions of $\hat{\Lambda} \cdot \hat{n}$ for the combined data sample discussed above. Moments computed from the I_Λ (intensity) and the $IP_\Lambda \cdot \hat{\Lambda}$ (longitudinal polarization) distributions were used to calculate the smooth curves on the four plots. The spin factor $(2J+1)$ accounts for most of the difference between the solid (spin $\frac{1}{2}$ assumed) and the dashed

(spin- $\frac{3}{2}$) curves on the $IP_\Lambda \cdot \hat{y}$ and $IP_\Lambda \cdot \hat{x}$ (transverse polarization) plots. The spin- $\frac{3}{2}$ assumption is not required and in fact is seen to fit the $(IP_\Lambda \cdot \hat{x})$ distribution somewhat worse than does $J = \frac{1}{2}$.

The resulting values of $2J+1$ from each of the four individual samples and from the combined samples are indicated by the vertical arrows (labeled as to sample) in Fig. 12. The smooth curves in the figure are the expected probability distributions for $2J+1$ for the various Ξ spin assumptions, and are calculated from the experimental moments and errors, as discussed below.

With the $\beta_z t_{10}$ moment omitted from the numerator and with the denominator calculated as above, the square root of the right side of (5.6) can be represented as the ratio of two approximately normally distributed quantities. One can compute the distribution function for this ratio subject to each spin assumption, given an estimate of t_{10} and the moment variance matrix.²⁰ These probability distributions for spins $\frac{1}{2}$ and $\frac{3}{2}$, together with the experimental results, are displayed in Fig. 12 for each of the four subsamples and for the combined, rotated sample. The fractional area under a particular $J = \frac{3}{2}$ curve to the left of the corresponding experimental point represents the confidence level on the assumption that the spin factor is that small, or smaller. We observe that only subsample D yields much discrimination against spin $\frac{3}{2}$. For the combined sample, with α_z ranging from -0.48 to -0.34 , the spin- $\frac{3}{2}$ confidence levels range from 0.15 down to 0.02. The related confidence levels, calculated from the spin- $\frac{1}{2}$ curves, that a result be as large as or larger than the experimental point, range from 0.22 to 0.42. For an assumed spin of $\frac{5}{2}$, the confidence level ranges from 0.003 to 0.0002.

D. Maximum-Likelihood Analysis

An alternative method to the ratio test is the maximum likelihood method. Here, in order to determine directly the relative confidence levels for the competing spin hypotheses, and to obtain best values for the decay parameters, we re-analyzed the data via a procedure in which the statistical contribution from each subsample

²⁰ As discussed by N. Byers (private communication), the probability of finding A in some interval dA , for $A=Y/X$, is

$$P(A)dA = dA \int Q(AX)R(X) \frac{\partial(A, X)}{\partial(A, X)} dX.$$

With Y and X assumed to obey Gaussian distributions $Q(Y)$ and $R(X)$, and with ϵ representing the error matrix for Y and X, the probability of finding A (if the true value of spin is J, if A has a mean value of $(2J+1)$, and if X_0 and the ϵ components are given by experimental analysis) is

$$P[A; (2J+1)] = [(\det \|\epsilon^{-1}\|)^{1/2} / 2\pi] \int_0^\infty X dX [e^{-z^2} + e^{-z}],$$

where

$$\begin{aligned} Z_\pm[A, (2J+1)] = & -(\frac{1}{2}(\epsilon^{-1})_{XX}[X^2 + X_0^2 \mp 2XX_0] \\ & + \frac{1}{2}(\epsilon^{-1})_{YY}[A^2 X^2 + (2J+1)^2 X_0^2 \mp 2A(2J+1)XX_0] \\ & + \frac{1}{2}(\epsilon^{-1})_{XY}[AX^2 + (2J+1)X_0^2 \mp [A + (2J+1)]XX_0]). \end{aligned}$$

TABLE IV. Bin-selection criteria for the maximum-likelihood decay analysis. The tabulated figures are from a fit with independent information on α_Λ and $(\alpha_\Lambda\alpha_\Xi)$ included as in (5.10).

Bin	P_{beam} (BeV/c)	Angular interval ^a	N	$J = \frac{1}{2}$ polarization	$J = \frac{3}{2}$ fit parameters			Constraint violated
					$(\frac{2}{5})^{1/2}t_{10}$	$(\frac{1}{5})^{1/2}t_{20}$	$(7/5)^{1/2}t_{30}$	
Ξ^- data								
1	1.2	all	33	-0.95 ± 0.36	-0.48 ± 0.24	0.30 ± 0.40	-0.18 ± 0.70	5.12a
2	1.3	$x < 0$	25	0.02 ± 0.44	$+0.01 \pm 0.30$	0.36 ± 0.46	0.82 ± 0.86	
3		$x > 0$	62	-0.78 ± 0.26	-0.45 ± 0.17	-0.26 ± 0.27	0.51 ± 0.47	5.12b
4	1.4	$x < 0$	26	1.00 ± 0.32	0.61 ± 0.19	-0.62 ± 0.40	-0.85 ± 0.59	5.12c
5		$x > 0$	49	-0.83 ± 0.35	-0.54 ± 0.23	0.24 ± 0.32	0.97 ± 0.62	5.12a
6	1.5	$x < -0.2$	120	0.89 ± 0.20	0.61 ± 0.14	-0.52 ± 0.19	-0.07 ± 0.36	5.12c
7		$-0.2 < x < 0.3$	83	-0.20 ± 0.27	-0.13 ± 0.19	0.15 ± 0.27	0.41 ± 0.47	
8		$0.3 < x < 0.75$	120	-0.51 ± 0.23	-0.33 ± 0.16	0.04 ± 0.20	0.31 ± 0.40	
9		$x > 0.75$	145	-0.21 ± 0.19	-0.19 ± 0.13	0.03 ± 0.18	0.10 ± 0.34	
10	1.6	$x < 0$	24	0.75 ± 0.33	0.91 ± 0.43	0.94 ± 0.41	-0.01 ± 0.88	5.12d
11		$x > 0$	36	0.11 ± 0.43	-0.07 ± 0.31	-0.31 ± 0.33	-0.21 ± 0.71	
12	1.7	all	105	0.64 ± 0.22	0.29 ± 0.16	0.42 ± 0.23	-0.48 ± 0.40	5.12d
Ξ^0 data								
13	all	all	146	-0.64 ± 0.22^b -0.52 ± 0.20^c				
Total ΞK events 974								

^a $x = (\hat{\mathbf{K}}^- \cdot \hat{\mathbf{\Xi}})$, cascade production cosine (c.m.) in the reaction.

^b α_{Ξ^0} and Φ_{Ξ^0} determined independently.

^c α_{Ξ^0} and Φ_{Ξ^0} assumed equal to α_{Ξ^-} and Φ_{Ξ^-} .

was estimated separately (and the polarization parameters were optimized separately). Equations (5.5) give, for some particular odd- L , M value, conditions on the parameters J , α_Ξ , Φ_Ξ , and t_{LM} . Fixing the value of one or more of these leaves the system overdetermined and allows calculation of the consistency of the data with the assumed values. Application of conditions (5.5) to other subsamples increases the redundancy, because the decay parameters are common to all the different subsamples and orders of L ; only the t_{LM} are new.

1. Spin- $\frac{1}{2}$ Analysis

The distribution function describing the observation of the sequential Ξ and Λ decays may be written in terms of (5.3) as

$$\mathcal{P} = [I_\Lambda(\theta, \phi) + \alpha_\Lambda(I_\Lambda \mathbf{P}_\Lambda) \cdot \hat{\mathbf{p}}]. \quad (5.7)$$

The fit of spin assumption $J = \frac{1}{2}$ to a particular data sample consists of maximizing the logarithm of the likelihood function [which derives from the distribution function (5.7)]

$$w(J = \frac{1}{2}) = \ln \prod_{k=1}^N \mathcal{P}_k(\theta_k, \phi_k, \hat{\mathbf{p}}_k; \alpha_\Xi, \Phi_\Xi, t_{10}), \quad (5.8)$$

subject to variations in the decay parameters α_Ξ and Φ_Ξ , and the initial-state parameter t_{10} . As noted above, the full sample must be decomposed into various production energy and angle bins to obtain subsamples characterized by nonzero t_{10} . We split the data at each production energy into new angular subsamples as long as the increase in the best-fit likelihood was somewhat larger than expected *a priori*.²¹ Omission of any one of

²¹ With the inclusion into the fit of N new parameters, each capable of unconstrained variation, one would expect the logarithm of the best-fit likelihood to increase by $N/2$ if the dependence

of the true distribution function on these parameters were random. An increase of substantially more than this figure would indicate that one (or more) of the new parameters satisfied some requirement of the data and was therefore statistically quite different from zero. The imposition of constraints [for example, (5.12)] on the free variation of the new parameters, would of course reduce the range of variation of these parameters and might lead to an increase in the likelihood rather less than indicated.

Additional information on the parameters α_Λ and α_Ξ from two different sources was utilized in the fitting process. The data from the 176 Ξ^- decays from deuterium productions and three-body productions were included by adding to (5.8) a term of the form

$$w_1 = \sum_{k=1}^{176} \ln [1 + \alpha_\Lambda \alpha_\Xi (\hat{\Lambda} \cdot \hat{\mathbf{p}})_k], \quad (5.9)$$

and the measurements from independently published experiments^{19,22} were included by adding a further term of the form

$$w_2 = -\frac{1}{2} \left\{ \left(\frac{\alpha_\Lambda - 0.62}{0.07} \right)^2 + \left(\frac{\alpha_\Lambda \alpha_{\Xi^-} + 0.32}{0.048} \right)^2 \right\} \quad (5.10)$$

²² J. Cronin and O. Overseth, Phys. Rev. **129**, 1795 (1963).

TABLE V. Best-fit values for the decay parameters. Columns 1 and 5 list our best-fit independent determinations of the cascade nonleptonic decay parameters α_{Ξ} and Φ_{Ξ} (in radians) ($=\tan^{-1}(\beta/\gamma)_{\Xi}$). Columns 2 and 6 are averages of our numbers together with published results tabulated in Ref. 19; the entries in column 6 result from combining the Ξ^{-} and Ξ^0 data, assuming $\alpha_{\Xi^{-}}=\alpha_{\Xi^0}$, $\Phi_{\Xi^{-}}=\Phi_{\Xi^0}$. Columns 3 and 4 indicate the stability of the results against reasonable variations in α_{Λ} .

Independent information	α_{Λ}	0.62 ± 0.07	0.62 ± 0.07	Ξ^{-}	free	Ξ^0	0.62 ± 0.07	$\Xi^{-}+\Xi^0$	0.62 ± 0.07
	$(\alpha_{\Lambda}\alpha_{\Xi})$	free	-0.321 ± 0.048	free	free	free	-0.321 ± 0.048	-0.321 ± 0.048	
$w=\ln \mathcal{L}$		38.65	37.85		38.74		5.01		40.93
Decay-parameter results	α_{Λ}	0.641 ± 0.056	0.662 ± 0.052	0.682 ± 0.104	0.726 ± 0.096	0.627 ± 0.07	0.669 ± 0.052		
	α_{Ξ}	-0.368 ± 0.057	-0.410 ± 0.047	-0.362 ± 0.058	-0.389 ± 0.053	-0.149 ± 0.154	-0.389 ± 0.045		
	Φ_{Ξ}	0.008 ± 0.186	0.008 ± 0.188	0.006 ± 0.185	0.005 ± 0.183	-0.05 ± 0.41	-0.003 ± 0.172		
	$(\delta_P-\delta_S)$	179 ± 26 deg.							
Correlation coefficients	$C(\alpha_{\Lambda}\alpha_{\Xi})$	0.096	0.344	0.295	0.623	-0.058	0.329		
	$C(\alpha_{\Lambda}\Phi_{\Xi})$	0.014	0.015	0.027	0.029	0.003	0.013		
	$C(\alpha_{\Xi}\Phi_{\Xi})$	0.007	0.011	0.015	0.022	-0.064	0.004		

to the likelihood logarithm. Published results on Φ_{Ξ} do not include the $\langle\alpha_{\Xi^{-}},\Phi_{\Xi^{-}}\rangle$ correlation coefficient, and so information on this parameter was not included. The Ξ^0 data were treated in the same way; two-body events were lumped into one bin and characterized with a function of the form (5.8), the $\Xi^0 K^+\pi^-$ were included as in (5.9), and the Ξ^0 and Λ decay asymmetries were inserted by inclusion of a term

$$-\frac{1}{2}\left\{\left(\frac{\alpha_{\Lambda}-0.62}{0.07}\right)^2+\left(\frac{\alpha_{\Lambda}\alpha_{\Xi^0}+0.07}{0.21}\right)^2\right\}.$$

Our best-fit results for the Ξ decay parameters (assuming $J_{\Xi}=\frac{1}{2}$) are summarized in Table V. The first four columns list Ξ^{-} results under various combinations of restrictions (5.10); our results, independent of other cascade data, are those of column 1. The fifth column gives our results for the Ξ^0 . The sixth column lists the results of analyzing the Ξ^{-} and Ξ^0 simultaneously under the assumption that the Ξ^{-} and Ξ^0 decay parameters are equal.

2. Spin- $\frac{3}{2}$ Analysis

Analysis of the Ξ^{-} decay data under the $J=\frac{3}{2}$ spin assumption proceeds as above, except for inclusion of six new initial-state parameters per data subsample into the distribution function, viz., t_{20} , t_{30} , and the real and imaginary parts of t_{22} and t_{32} . With the same decomposition of the complete data into 12 bins employed above in the spin- $\frac{1}{2}$ case, this implies the introduction of the somewhat unmanageable number of 72 new parameters.

The expansion polynomials Y_{LM} and \mathcal{D}_{M1}^L depend harmonically on the azimuthal angle Φ_{Λ} ; averaging over this angle thus removes from the distribution function all terms with $M\neq 0$. Expanding (5.7) and performing the azimuthal averaging, we obtain

$$\mathcal{P}=[1+\alpha_{\Lambda}\alpha_{\Xi}(\hat{\Lambda}\cdot\hat{p})]S(\cos\theta)+(\alpha_{\Xi}+\alpha_{\Lambda}\hat{\Lambda}\cdot\hat{p})T(\cos\theta)+\frac{1}{2}(2J+1)\alpha_{\Lambda}(\beta_{\Xi}\hat{y}\cdot\hat{p}-\gamma_{\Xi}\hat{x}\cdot\hat{p})U(\cos\theta), \quad (5.11a)$$

where

$$S(\cos\theta)=1+\sum_{L=2}^{2J}E_L4\pi\left(\frac{2L+1}{4\pi}\right)^{1/2}\times(n_{L0}^J t_{L0})P_L(\cos\theta), \quad (5.11b)$$

$$T(\cos\theta)=\sum_{L=1}^{2J}O_L4\pi\left(\frac{2L+1}{4\pi}\right)^{1/2}\times(n_{L0}^J t_{L0})P_L(\cos\theta), \quad (5.11c)$$

and

$$U(\cos\theta)=\sum_{L=1}^{2J}O_L\frac{4\pi}{L(L+1)}\left(\frac{2L+1}{4\pi}\right)^{1/2}\times(n_{L0}^J t_{L0})P_L^1(\cos\theta). \quad (5.11d)$$

This procedure reduces the number of new parameters per bin from 6 to 2 (t_{20} and t_{30}). If the spin of the Ξ were truly $\frac{3}{2}$, the removal of the terms t_{22} and t_{32} could reduce our statistical discrimination against spin $\frac{1}{2}$. [In analyses of the spin of the $\Xi^*(1530)$, these terms were in fact important in determining that $J\geq\frac{3}{2}$.¹⁰] Ignoring these should not, however, bias the results in favor of spin $\frac{1}{2}$ with respect to $\frac{3}{2}$. We may lose statistical precision, but we gain a reduction in the number of additional initial-state parameters needed to describe the spin- $\frac{3}{2}$ case from 72 to 24. Thus our spin- $\frac{3}{2}$ analysis involves a 39-parameter fit to the data.

The diagonal elements of the density matrix (5.2) are required to be nonnegative. These requirements impose spin-dependent restrictions on the maximum permissible magnitudes of the t_{L0} , which must be imposed while seeking optimal sets of the parameters in order to obtain physically meaningful values. For spin $\frac{1}{2}$, this constraint is equivalent to requiring that the magnitude of the polarization of each subsample be less than 1. For the spin- $\frac{3}{2}$ fit, the following conditions

are obtained on the t_{L0} in each sample bin²³:

$$1 + \frac{3}{\sqrt{5}}(\sqrt{3}t_{10}) + (5^{1/2}t_{20}) + \frac{1}{\sqrt{5}}(7^{1/2}t_{30}) \geq 0, \quad (5.12a)$$

$$1 + \frac{1}{\sqrt{5}}(\sqrt{3}t_{10}) - (5^{1/2}t_{20}) - \frac{3}{\sqrt{5}}(7^{1/2}t_{30}) \geq 0, \quad (5.12b)$$

$$1 - \frac{1}{\sqrt{5}}(\sqrt{3}t_{10}) - (5^{1/2}t_{20}) + \frac{3}{\sqrt{5}}(7^{1/2}t_{30}) \geq 0, \quad (5.12c)$$

$$1 - \frac{3}{\sqrt{5}}(\sqrt{3}t_{10}) + (5^{1/2}t_{20}) - \frac{1}{\sqrt{5}}(7^{1/2}t_{30}) \geq 0. \quad (5.12d)$$

We note that the distribution function may remain positive over a wider range of the t_{L0} than indicated by the physical limits (5.12) because of the particular values assumed by the decay parameters.

If the spin of the cascade is indeed unexpectedly $\frac{3}{2}$, our best fits for the decay parameters [subject to constraints (5.12) and including the information of (5.10)] are $\alpha_A(J_Z = \frac{3}{2}) = +0.654 \pm 0.060$, $\alpha_Z(J_Z = \frac{3}{2}) = -0.428 \pm 0.062$, and $\Phi_Z(J_Z = \frac{3}{2}) = -0.024 \pm 0.210$ rad. We see by comparison with the entries of Table V that these quantities are not strongly spin-dependent.

3 Comparison of Results

Comparisons among fits to the data of the competing hypotheses $J = \frac{1}{2}$ and $J = \frac{3}{2}$ involve the examination of three effects:

(a) Addition of the 24 parameters t_{20} and t_{30} in the spin- $\frac{3}{2}$ fit allows description both of more complex angular distributions and of minor statistical fluctuations. Even if all these t_{L0} were truly zero, we should expect a fit with them to give an approximate increase in the logarithm of the likelihood of 12 over the spin- $\frac{3}{2}$ fit with t_{10} varied but t_{20} and t_{30} constrained to be zero.²¹

(b) The distribution function (5.11a) depends explicitly on the spin factor $(2J+1)$. Ignoring questions of the order of the complexity of the angular distributions, we hope to see a decrease in the likelihood as the spin is varied from the correct to the incorrect value.

(c) The fit of the spin- $\frac{3}{2}$ hypothesis to the data may yield (in one or more bins) values of the t_{L0} that violate one of the linear inequalities (5.12). We perform fits first requiring only that the distribution function remain positive, then apply the constraints (5.12) and re-optimize the fits to study the effect of such violations.

In Table VI are tabulated best-fit likelihood logarithm results for various combinations of assumptions on the spin and complexity of the angular distributions.

²³ These constraints are closely related to the conditions developed by T. D. Lee and C. N. Yang [Phys. Rev. **109**, 1755 (1958)]. In particular, if $t_{20} = t_{30} = 0$, one can easily see that (5.12a) and (5.12d) combine to give the restriction $(\cos\theta_A) \leq 1/9 = 1/6J$, for $J = \frac{3}{2}$.

TABLE VI. Maximum-likelihood spin-analysis results. The table entries are the logarithms of the maximum-likelihood solution. The normalization is such that complete isotropy (zero polarization or alignment) would give a result of zero. Fits (A) included independent measurements of α_A and $(\alpha_A\alpha_Z)$ as in (5.10); fits (B) included independent measurements of α_A only. Results for $(2J+1) = 4$ are given both with and without the density-matrix constraints of (5.12).

L_{\max}	No. parameters	Fit	$(2J+1) = 4$		
			$(2J+1) = 2$	Unconstrained	Constrained
1	15	(A)	37.85	35.62	31.95
1	15	(B)	38.65	36.05	32.34
3	39	(A)	51.63	50.09	45.20
3	39	(B)	52.36	50.71	45.64

These results, in contrast to those of the ratio test, are quite insensitive to variations in α_A , α_Z , and Φ_Z . Fits (A) result from including independent information on both α_A and $(\alpha_A\alpha_Z)$ as in (5.10); fits (B) had only α_A information. The entries of column 1 in the table are results of fits with $(2J+1) = 2$ (spin $\frac{1}{2}$), whereas those of columns 2 and 3 had $(2J+1) = 4$. The results in column 2 are from fits where the t_{L0} parameters were allowed to vary freely as long as the distribution function remained positive. The constraints (5.12) were imposed on the t_{L0} in each bin for the results given in column 3. Results in rows 1 and 2 are from the 15 parameter fits (α_A , α_Z , Φ_Z , and 12 separate t_{10}) to the assumption that the maximum order in the angular distributions (5.6) was $L_{\max} = 1$; results in rows 3 and 4 are from the 39-parameter fits to the assumption $L_{\max} = 3$.

The increase in likelihood between corresponding fits (i.e., same column, same decay-parameter information) from $L_{\max} = 1$ to $L_{\max} = 3$ we attribute to the first effect discussed above; we observe approximately the increase we had expected *a priori*. We conclude that our experimental determinations of the higher order terms are completely consistent with the hypothesis that these are truly zero. The decrease in likelihood of corresponding fits from column 1 to column 2 we attribute to effect (b), the sensitivity to the spin factor $(2J+1)$. We interpret the average logarithmic decrease of 2 as equivalent to a (one-dimensional) $\chi^2 \approx 4$, corresponding to a confidence level of 5% for the hypothesis $J = \frac{3}{2}$ as compared to the hypothesis $J = \frac{1}{2}$. The decrease in likelihood from fit results of column 2 to the corresponding column-3 results we attribute to effect (c), the imposition of the density-matrix constraints. If these constraints were violated in a statistically convincing way, we would interpret this as evidence against spin $\frac{3}{2}$. In seven of our 12 bins, the unconstrained fit estimates for the t_{L0} violated one of the constraints (5.12). The average logarithmic likelihood decrease of ~ 5 we interpret as a 7-constraint $\chi^2 \approx 10$, and represents the statistical amount we have to stretch the fits of column 2 to reach the nearest physically meaningful solution. The corresponding confidence

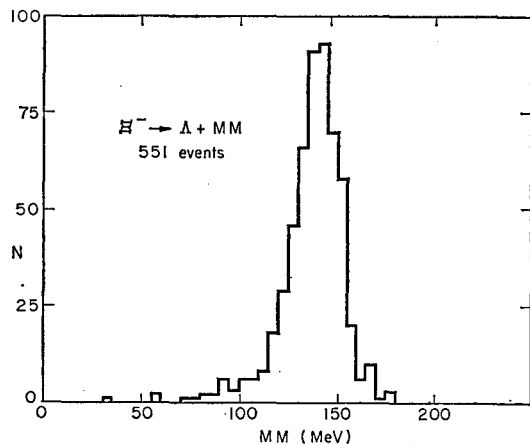


FIG. 13. Mass recoiling from Λ : $\Xi^- \rightarrow \Lambda + (MM)$.

level of 15% demonstrates that we have no statistically convincing evidence for violation of the density-matrix constraints.

We may estimate the minimum expected variance of the spin factor $(2J+1)$ (as a function of the decay parameters and Ξ polarization) from the distribution function.²⁴ We find that, for a sample of Ξ decays characterized by $|\langle P_{\Xi} \rangle| = 0.5$, we would require at least 750 events to yield a variance approximately equivalent to a four-standard-deviation result (if the best-fit value of $2J+1$ is less than 2). This variance estimate scales approximately as $(N^{1/2} |\langle P_{\Xi} \rangle|)^{-1}$.

E. Spin and Nonleptonic Decay-Analysis Results

Our conclusion from the spin analysis of our data is that the confidence level for the hypothesis $J_{\Xi} = \frac{3}{2}$ is 5% of that for the hypothesis $J_{\Xi} = \frac{1}{2}$, equivalent approximately to a two-standard-deviation result. Hereinafter, we shall assume $J_{\Xi} = \frac{1}{2}$; in particular, we write $S = A_{J-1/2}$ and $P = A_{J+1/2}$ for the decay amplitudes of (5.1).

Our best fits for both Φ_{Ξ^-} and Φ_{Ξ^0} yield values less in magnitude than $\pi/2$; thus $\gamma_{\Xi} > 0$, and the cascade decay is seen to proceed mostly through S wave. In both Ξ^- and Ξ^0 cases we have searched for secondary solutions with Φ_{Ξ} constrained to be greater than $\pi/2$ (and thus $\gamma_{\Xi} < 0$). For the Ξ^- , the best such solution is worse by more than seven standard deviations than the solution given. For the Ξ^0 , the limited statistics allow only a two-standard-deviation distinction between the $\gamma_{\Xi^0} > 0$ and $\gamma_{\Xi^0} < 0$ solutions.

Our result $\alpha_{\Xi} = -0.368 \pm 0.057$ is clearly inconsistent with zero and, thus, with parity conservation in the Ξ decay process. The phase angle $(\delta_+ - \delta_-) = (\delta_P - \delta_S)$ defined in Eqs. (5.1) may be computed from the values

of α_{Ξ} and Φ_{Ξ} ; we find for the Ξ^-

$$(\delta_P - \delta_S) = \tan^{-1}(\beta/\gamma)_{\Xi} = \tan^{-1}[\sin\Phi_{\Xi}(1 - \alpha_{\Xi}^2)^{1/2}/\alpha_{\Xi}] = 179 \pm 26 \text{ deg.} \quad (5.14)$$

This result is consistent with T invariance of the original decay transition together with a small $\Lambda\pi$ final-state scattering phase shift. Invariance under C would require a $\Lambda\pi$ phase shift near $\pi/2$ in magnitude. There is no known $\Lambda\pi$ resonance with spin $\frac{1}{2}$ near the invariant mass 1320 MeV [even if J_{Ξ} is $\frac{3}{2}$, the known $Y_1^*(1385)$ should introduce a $\Lambda\pi$ phase shift of not more than about 20 deg]; we deem highly unlikely a $\Lambda\pi$ -scattering phase shift of nearly 90 deg and conclude that our result is consistent with T invariance and inconsistent with C invariance in the Ξ decay.

The assumption that the decay amplitudes obey the $\Delta I = \frac{1}{2}$ rule leads to the prediction that $S_{\Xi^0} = -(1/\sqrt{2})S_{\Xi^-}$ and $P_{\Xi^0} = -(1/\sqrt{2})P_{\Xi^-}$ and thus $\alpha_{\Xi^0} = \alpha_{\Xi^-}$, $\Phi_{\Xi^0} = \Phi_{\Xi^-}$ for the decay parameters, and $\lambda_{\Xi^0} = 2\lambda_{\Xi^-}$ for the decay rates. Combining our earlier result that $(\lambda_{\Xi^0}/\lambda_{\Xi^-}) = 0.68 \pm 0.10$ with the result obtained by comparing the results of the fits in columns 2, 5, and 6 of Table V, we find that our results are consistent with the $\Delta I = \frac{1}{2}$ predictions with a confidence level of 22%.

VI. SEARCH FOR LEPTONIC DECAYS

The search for $|\Delta S| = 1$ leptonic decay modes of the Ξ^- was restricted to $\Xi^- K^+$ production events with a visible Λ decay. The topology ($\Xi^- \rightarrow \Lambda + X^- + \text{neutrals}$) can include the following decay modes:

$$\Xi^- \rightarrow \Lambda + \pi^-, \quad (A)$$

$$\Xi^- \rightarrow \Lambda + \pi^- + \gamma, \quad (B)$$

$$\Xi^- \rightarrow \Lambda + e^- + \bar{\nu}, \quad (C)$$

$$\Xi^- \rightarrow \Lambda + \mu^- + \bar{\nu}, \quad (D)$$

$$\Xi^- \rightarrow \Sigma^0 + e^- + \bar{\nu}, \quad \Sigma^0 \rightarrow \Lambda + \gamma, \quad (E)$$

$$\Xi^- \rightarrow \Sigma^0 + \mu^- + \bar{\nu}, \quad \Sigma^0 \rightarrow \Lambda + \gamma. \quad (F)$$

A fiducial volume was chosen to allow at least 12 cm of beam track and to eliminate regions of the bubble chamber near the walls where turbulence makes accurate observation and measurement difficult. About 20% of the effective chamber volume was removed by these restrictions. In addition, the lengths of the Ξ^- and Λ hyperons were each required to be at least 0.5 cm. Finally, about 10% of the events were discarded because either the $\Xi^- K^+$ -production fit or the Λ -decay fit had an unusually large χ^2 . This restricted sample contained 551 events.

Information on the leptonic decay modes was obtained (a) from the spectrum of the mass recoiling from the Λ , and (b) from the ionization of the X^- .

The missing-mass spectrum, $\Xi^- \rightarrow \Lambda + (MM)$, is shown in Fig. 13. Figure 14 displays $\eta = [(MM)^2 - M_{\pi}^2]/$

²⁴ See, for instance, Frank, T. Solmitz, *Ann. Rev. Nucl. Sci.* **14**, 375 (1964), Eq. (25).

$[\delta(MM)^2]$ the number of standard deviations from the π^- mass. From a sample of 551 events we would expect about 1.5 events with $|\eta| > 3$ and 1/30 event with $|\eta| > 4$. Two events with $|\eta| > 4$ were observed. One of these events is clearly pionic, as the π^- is observed to charge-exchange. We do not fully understand this event, since it fails to give a satisfactory fit to either pionic decay mode (A) or (B); it is definitely not a leptonic Ξ^- decay and will not be considered further here. The second event gives poor fits with comparable confidence levels to the normal pionic decay (A) and to the leptonic decay modes (C) and (D); it is inconsistent with the leptonic decay modes (E) and (F), because the laboratory momentum of the X^- is higher than the maximum allowed for these modes. This event is a very unlikely candidate for leptonic decay; however, we include it as an upper limit for leptonic decay modes (C) and (D). We conclude from this analysis that we have no examples of decay modes (E) and (F) and that there is not more than one example of decay modes (C) and (D) in the effective sample.

The effective sample size appropriate to this missing-mass analysis is obtained by removing the phase space within four standard deviations of the π^- mass. The expected mass spectrum for leptonic decay varies appreciably with the degree of correlation between the lepton and the neutrino. The parameter $\alpha = (|C_V|^2 - |C_A|^2) / (|C_V|^2 + 3|C_A|^2)$ in the angular correlation expression $w(\theta_{e\bar{\nu}}) = 1 + \alpha(v/c) \cos\theta_{e\bar{\nu}}$ is obviously limited by $-\frac{1}{3}$ and $+1$; in particular, α is zero for a pure $(V-A)$ interaction.²⁵ Cabibbo's theory of leptonic decays, based on octet dominance in SU_3 , indicates $\alpha \approx +1$ for the Λ modes (C) and (D), and $\alpha \approx 0$ for the Σ^0 modes (E) and (F).²⁶ The efficiencies for detecting modes (C), (D), (E), and (F) are 40, 15, 30, and 40%, respectively.

We have attempted to improve the detection efficiency for the electronic decay modes by positive identification of the e^- by ionization. All events with X^- momentum less than 100 MeV/c in the laboratory and with dip angle less than 60 deg have been investigated for ionization. (A π^- at 100 MeV/c is about three times as dark as a minimum ionizing e^- .) Events with tracks at dip angles larger than 60 deg have been rejected, since the linear bubble density increases by more than a factor of 2 over flat tracks, due to the projection onto the film plane.

Of the 551 Ξ^-K^+ events, 83 have X^- laboratory momentum less than 100 MeV/c; 74 of the latter events have dip angles less than 60 deg. None of these events have ionization consistent with the e^- hypothesis.

There are two events with the topology of Ξ^- production and decay in which the X^- are obviously electrons. These events have been identified as $\Sigma^- \rightarrow \Lambda + e^-$

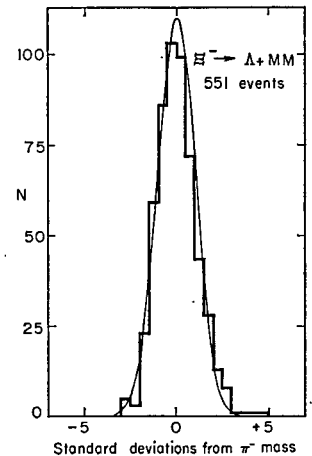


FIG. 14. Standard deviations from π^- mass: $\eta = [(MM)^2 - M_{\pi}^2] / [\delta(MM^2)]$. The smooth curve represents a normal error distribution. The missing-mass errors were increased by a factor of 1.25 due to the excess width of the χ^2 distributions.

$+ \bar{\nu}$. Neither of these events gave an adequate fit to the Ξ^-K^+ production hypothesis; thus they were not candidates for this analysis.

The electron momentum spectrum expected from our Ξ^- data has been calculated. Conservation of parity in the production process ensures that any net Ξ polarization be along the normal to the production plane (assuming $J_{\Xi} = \frac{1}{2}$). No correlation is then allowed between the electron direction in the Ξ rest frame and the Ξ direction in any frame. Thus the laboratory momentum spectrum, as well as the spectrum in the rest frame, is independent of the relative strengths of the vector and axial-vector couplings (i.e., independent of α). The rest frame spectrum is $\mathcal{P}(E, \mu) dE d\mu = PE(Q-E)^2 \times dE d\mu$, where P and E are, respectively, the rest-frame momentum and energy of the electron, Q is the difference between the initial- and final-state baryon masses, and μ is the cosine of its angle with the Ξ laboratory direction. The laboratory spectrum is obtained by Lorentz-transforming this spectrum and integrating over μ .

The ionization analysis is sensitive to 30% of the $\Xi^- \rightarrow \Lambda e^- \bar{\nu}$ events and 55% of the $\Xi^- \rightarrow \Sigma^0 e^- \bar{\nu}$ events. This result represents an increase detection efficiency for decay mode (E).

The upper limits for the $|\Delta S| = 1$ leptonic Ξ^- decay modes are

$$\begin{aligned} R_C(\Xi^- \rightarrow \Lambda e^- \bar{\nu}) &\leq 1/(0.4 \times 551) \approx 0.5\%, \\ R_D(\Xi^- \rightarrow \Lambda \mu^- \bar{\nu}) &\leq 1/(0.15 \times 551) \approx 1.2\%, \\ R_E(\Xi^- \rightarrow \Sigma^0 e^- \bar{\nu}) &< 1/(0.55 \times 551) \approx 0.3\%, \\ R_F(\Xi^- \rightarrow \Sigma^0 \mu^- \bar{\nu}) &< 1/(0.4 \times 551) \approx 0.5\%. \end{aligned}$$

The film was searched for $|\Delta S| = 1$ leptonic decay modes of the Ξ^0 with $\Delta S/\Delta Q = +1$,

$$\Xi^0 \rightarrow \Sigma^+ + e^- + \bar{\nu}, \quad (G)$$

$$\Xi^0 \rightarrow \Sigma^+ + \mu^- + \bar{\nu}, \quad (H)$$

²⁵ E. J. Konopinski, Ann. Rev. Nucl. Sci. 9, 99 (1959).

²⁶ Nicola Cabibbo, Phys. Rev. Letters 10, 531 (1963).

TABLE VII. Covariant nonleptonic decay amplitudes. Information on the non- Ξ^- data was taken from A. H. Rosenfeld *et al.*, Rev Mod. Phys. 37, 633 (1965). Column (a) under the Ξ^- lists our independent results; column (b) contains the average of these results with the world compilation of Ref. 19. Results are given for the two possible signs of γ for the Σ_0^+ decay.

	Ξ^-		Λ^-	Σ_0^+	
	a	b		$\gamma_{\Sigma} < 0$	$\gamma_{\Sigma} > 0$
$\tau \times 10^{10}$ sec	1.69 \pm 0.07	1.75 \pm 0.05	2.62 \pm 0.03	0.794 \pm 0.023	0.794 \pm 0.023
branching function	1.00	1.00	0.660 \pm 0.004	0.507 \pm 0.023	0.507 \pm 0.023
$\lambda \times 10^{-10}$ sec $^{-1}$	0.592 \pm 0.025	0.571 \pm 0.018	0.252 \pm 0.03	0.639 \pm 0.036	0.639 \pm 0.036
α	-0.368 \pm 0.056	-0.410 \pm 0.048	0.662 \pm 0.052	-0.90 \pm 0.25	-0.90 \pm 0.25
$(1-\alpha^2)^{1/2}$	0.9298	0.9121	0.7495	0.4395	0.4395
$\epsilon = B / A $	3.08 \pm 0.51	3.46 \pm 0.43	7.10 \pm 0.74	6.28 \pm 4.0	15.99 \pm 10.2
$A \times 10^{-5} \mu^{-1}$ sec $^{-1}$	2.064 \pm 0.045	2.018 \pm 0.032	1.512 \pm 0.021	2.67 \pm 1.22	1.05 \pm 0.19
$B \times 10^{-5} \mu^{-1}$ sec $^{-1}$	-6.36 \pm 1.02	-6.99 \pm 0.80	1.74 \pm 0.99	-16.8 \pm 3.1	-16.8 \pm 7.7
		($\Xi^- - \frac{1}{2}\Lambda^-$)		($\sqrt{\frac{2}{3}}\Sigma_0^+$)	
$A \times 10^{-5} \mu^{-1}$ sec $^{-1}$		1.262 \pm 0.034		2.312 \pm 1.1	0.9 \pm 0.2
$B \times 10^{-5} \mu^{-1}$ sec $^{-1}$		-12.36 \pm 0.95		-14.5 \pm 2.6	-14.5 \pm 6.7

and with $\Delta S/\Delta Q = -1$,

$$\Xi^0 \rightarrow \Sigma^- + e^+ + \nu, \quad (I)$$

$$\Xi^0 \rightarrow \Sigma^- + \mu^+ + \nu. \quad (J)$$

No serious candidates for these decay modes were discovered.

Upper limits are based on a sample of 106 $\Xi^0 K^0$ events within a restricted volume, corrected for neutral Λ decays. Minimum lengths for the Ξ^0 and Σ^\pm were set at 0.5 cm; these criteria would reject 25% of the Σ^+ events and 15% of the Σ^- events. The upper limits are

$$R_C(\Xi^0 \rightarrow \Sigma^+ e^- \bar{\nu}) < 1/(0.75 \times 1.5 \times 106) \simeq 0.9\%,$$

$$R_H(\Xi^0 \rightarrow \Sigma^+ \mu^- \bar{\nu}) < 1/(0.75 \times 1.5 \times 106) \simeq 0.9\%,$$

$$R_I(\Xi^0 \rightarrow \Sigma^- e^+ \bar{\nu}) < 1/(0.85 \times 1.5 \times 106) \simeq 0.8\%,$$

$$R_J(\Xi^0 \rightarrow \Sigma^- \mu^+ \bar{\nu}) < 1/(0.85 \times 1.5 \times 106) \simeq 0.8\%.$$

The only Ξ leptonic decays reported to date are examples of decay mode (C), $\Xi^- \rightarrow \Lambda e^- \bar{\nu}$. Carmony and Pjerrou observed one such event and report a branching ratio, $R_C \simeq 0.6\%$.²⁷ London *et al.* observed one definite and one probable leptonic Ξ^- in a restricted sample of 164 Ξ^- decays. Our result, $R_C \lesssim 0.5\%$, is not inconsistent with these published results.

VII. RESULTS BEARING ON PREDICTIONS FROM INTERNAL SYMMETRIES

Several authors have made predictions bearing on the decay and production of the Ξ hyperon.

The observed consistency of the full nonleptonic decay amplitudes with the Lee triangle,²⁸ $2\Xi^- = \Lambda^- + \sqrt{3}\Sigma_0^+$, was reported in Ref. 3. The decreased errors on our Ξ decay parameters do not affect this consistency, since the main uncertainty comes from the un-

²⁷ D. D. Carmony and G. M. Pjerrou, Phys. Rev. Letters 10, 381 (1963).

²⁸ Benjamin W. Lee, Phys. Rev. Letters 12, 83 (1964); Murray Gell-Mann, *ibid.* 12, 155 (1964); Hirotaka Sugawara, Progr. Theoret. Phys. (Kyoto) 31, 213 (1964).

certainty in the Σ_0^+ decay amplitudes. The covariant nonleptonic decay amplitudes A and B are related to the decay matrix and to the decay rate by

$$M = U(b')(A - B\gamma_5)U(b)$$

and

$$\lambda = \frac{1}{8\pi} \left(\frac{q}{\mu} \right) \left\{ \left[\frac{(M+m)^2 - \mu^2}{M^2} \right] |A|^2 + \left[\frac{(M-m)^2 - \mu^2}{M^2} \right] |B|^2 \right\}.$$

The U 's are the baryon spinors and M , m , and μ are the masses of the parent and decay baryons and the decay pion, while q is the c.m. decay momentum. We estimate the ratio $\epsilon = |B|/|A|$ from the decay parameters (5.1) (assuming $\beta = 0$) and obtain the normalization from the decay rates and branching ratios. These amplitudes are given in Table VII.

In the limit of SU_3 symmetry, the equality of certain production amplitudes is predicted.^{29,30} In particular, we have

$$A(K^- p \rightarrow \Xi^0 K^0) = A(K^- p \rightarrow \Sigma^- \pi^+), \quad (7.1a)$$

$$A(K^- n \rightarrow \Xi^- K^0) = A(\pi^- p \rightarrow \Sigma^- K^+), \quad (7.1b)$$

and

$$\begin{aligned} A(K^- p \rightarrow \Xi^{*-} K^+) &= A(\pi^- p \rightarrow Y_1^{*-} K^+) \\ &= -A(K^- p \rightarrow Y_1^{*-} \pi^+) \\ &= -(1/\sqrt{3})A(\pi^- p \rightarrow N^{*-} \pi^+). \end{aligned} \quad (7.1c)$$

According to the prescription of Meshkov, Snow, and Yodh,²⁹ the relativistically invariant amplitudes should be compared at equal Q values, so that the thresholds

²⁹ C. A. Levinson, H. J. Lipkin, and S. Meshkov, Phys. Letters 1, 44 (1962); S. Meshkov, C. A. Levinson, and H. J. Lipkin, Phys. Rev. Letters 10, 361 (1963); S. Meshkov, G. A. Snow, and G. B. Yodh, *ibid.* 12, 87 (1964).

³⁰ S. Meshkov, G. A. Snow, and G. B. Yodh, Phys. Rev. Letters 13, 212 (1964).

for additional channels coincide. The form given for the amplitude squared is $\bar{\sigma} = (E^{*2} p_{\text{in}} / p_{\text{out}}) \sigma$, where p_{in} and p_{out} are the c.m. momenta of incident and outgoing particles, and E^* is the total c.m. energy.

The available data allow an investigation of relation (7.1a) under the worst possible conditions, near threshold and far from the unitary limit. We study the endoergic reaction $K^- p \rightarrow \Xi^0 K^0$ from threshold ($Q=0$) to $Q=295$ MeV. This is to be compared with the exoergic reaction $K^- p \rightarrow \Sigma^- \pi^+$ ($Q=94$ MeV, even for K^- capture at rest). Furthermore, the $\Sigma^- \pi^+$ system passes through the $Y_0^*(1520)$ resonance at $Q=182$ MeV, with no known corresponding $\Xi^0 K^0$ resonant state. Comparing total cross sections, we find the ratio $\bar{\sigma}_{\Sigma^- \pi^+} / \bar{\sigma}_{\Xi^0 K^0} \sim 100$ at the lowest Q (135 MeV), falling to ~ 10 at $Q=295$ MeV.³¹ On the other hand, the differential cross sections are in excellent agreement at $Q=210$ MeV ($P_K=1.5$ BeV/c for $\Xi^0 K^0$ and 465 MeV/c for $\Sigma^- \pi^+$).

Relation (7.1b) provides a more favorable test of SU_3 predictions due to the kinematic similarity of the two reactions. At $Q=210$ MeV ($P_K=1.45$ BeV/c for $\Sigma^- K^+$),³² we obtain

$$\frac{\bar{\sigma}(K^- n \rightarrow \Xi^- K^0)}{\bar{\sigma}(\pi^- p \rightarrow \Sigma^- K^+)} = \frac{7.04 \times (165 \pm 34)}{6.39 \times (242 \pm 14)} = 0.75 \pm 0.16$$

Again the angular distributions are in reasonable agreement.

The compound prediction for Ξ^{*-} production, relation (7.1c), has been discussed in some detail by Meshkov *et al.*³⁰ The cross sections for reactions with final K are experimentally observed to be reduced in

magnitude by at least an order of magnitude relative to those with final π .

Inclusion of SU_6 symmetry provides additional relations among production amplitudes.³³ The ΞK production modes are related by

$$A(K^- p \rightarrow \Xi^0 K^0) = -A(K^- n \rightarrow \Xi^- K^0) \\ = -\frac{1}{2} A(K^- p \rightarrow \Xi^- K^+). \quad (7.2)$$

These relations are predicated on neglect of angular momenta and are most favorably studied near threshold, in contrast to the predictions of (7.1). Our results agree with (7.2) at the lower momenta ($Q \lesssim 200$ MeV). At 1.5 BeV/c and above, where most of the data lie, there is a clear inconsistency with the S -wave predictions of (7.2).

The relativistic completion of SU_6 predicts zero polarization in ΞK production. This prediction is inconsistent with the polarization data of Figs. 6 and 7, as remarked by Blankenbecler *et al.*³⁴

ACKNOWLEDGMENTS

We wish to thank Professor Harold K. Ticho and Professor Donald H. Stork for participation in the design and construction of the separated K^- beam. We are especially grateful to Margaret Alston and Peter Wohlmut for their work on the analysis of this experiment. We wish to express appreciation to Robert Watt and the crew of the 72-in. bubble chamber and to Thelonius Bonk and the other scanning and measuring personnel.

The support and encouragement of Professor Luis W. Alvarez is gratefully acknowledged.

³¹ M. B. Watson, M. Ferro-Luzzi, and R. D. Tripp, *Phys. Rev.* **131**, 2248 (1963); P. L. Bastien and J. P. Berge, *Phys. Rev. Letters* **10**, 188 (1963).

³² J. Adam Schwartz, Ph. D. thesis, Lawrence Radiation Laboratory Report No. UCRL-11360, 1964 (unpublished).

³³ J. C. Carter, J. J. Coyne, and S. Meshkov, *Phys. Rev. Letters* **14**, 523 (1965); V. Barger and M. H. Rubin, *ibid.* **14**, 713 (1965).

³⁴ R. Blankenbecler, M. L. Goldberger, K. Johnson, and S. B. Treiman, *Phys. Rev. Letters* **14**, 518 (1965).

